Steel Billet Through Heating: Experimental Validation Of Numerical Model EM-TH Coupled

Institut für Elektroprozesstechnik
Gottfried Wilhelm Leibniz Universität Hannover

Dipartimento di Ingegneria Elettrica
Università degli Studi di Padova

Master's Thesis
By
Boris Jelicic

Academic year: 2012-2013
Supervisor: Prof. Ing. Michele Forzan, Prof. Dr.-Ing. Egbert Baake
Assistant Supervisor: Dipl.-Ing. Sebastian Wipprecht, Dr.-Ing. Alexander Nikanorov

Index

Introduction 1
CHAPTER 1 – Induction theory 3
1.1 Electromagnetic Theory 3
1.2 Thermal Theory 10
CHAPTER 2 – Outlook of forging industry in Europe 15
2.1 Forging overlook in the UE 18
2.2 Forging in Germany 19
CHAPTER 3 – Forgings 21
3.1 Forging types 21
3.1.1 Die Forging 21
3.1.2 Flashless precision forging 21
3.1.3 Tool and machine technology 22
3.1.4 Application of precision forging with steel materials 23
3.1.5 Flash reduced forging technology 24
3.2 Induction reheating 26
CHAPTER 4 - Potential for saving of energy in forging industry 29
4.1 Energy consumption 29
4.2 Material savings 30
4.3 The project REForCh 32
4.3.1 Role of the ETP institute 33
CHAPTER 5 – Numerical analysis 35
5.1 Presentation of the studied system 35
5.1.1 The coils and the billet 35
5.1.2 Numerical model 38
5.1.3 Data recovery 40
5.2 First experiment 43
5.3 Second experiment 47
CHAPTER 6 – Application of the model 51
6.1 Simulations 51
6.1.1 D coils 51
6.1.2 C coils 55
6.1.3 Considerations 56
CHAPTER 7 – Final considerations 57
Appendix A – Symbols 59
Appendix B – Program 60
Appendix B1 Proprieties 60
Appendix B2 Harmonic electromagnetic analysis and transient thermal analysis 61
Appendix C – Electrical results 63
References 65

Introduction

Induction heating has become one of the main processes used for the heating of loads that are electrical conductors. This technique is widely used to heat metal prior to hot forming by forging, upsetting, extrusion and other processes.

In the last twenty years it has become the standard heating technology for die forging due to its ability to provide fast heating rates within the billet, high efficiency and productivity of the heating line, and repeatable high quality of heated work pieces while using a minimum of shop floor space. Further attractive features of induction heating is a noticeable reduction of scaling, little surface decarburisation and coarse-grain growth, short start-up and shut-down times and the ability to heat in a protective atmosphere. Nevertheless, the implementation of induction reheating into manufacturing processes for more complicated geometries, as for example crankshafts, is a new challenging task that has not been solved until now.

Because of the growing market and competitors, the European Union funded the REForCh (Resource Efficient Forging Process Chain for Complicated High Duty Parts) project which the main goal is to create an industrial forging process that improves the total efficiency and reduces the production of raw material, allowing economical benefits.

The goal is to create a numerical model that studies the evolution of the temperature inside the steel billet through induction heating. The model than has to be confirm after the comparison of the data on one of the machines in the Institut für Elektroprocesstechnik in Hannover.

If the numerical model is acting properly and answering correctly to the goals, than it will be adapted for the more complex production line process, like the one in REForCh.

Inside this script is explained: the theory of induction heating to better understand the results of the model, a study of the economy around the forging industries and the description and analysis on the data obtained through the virtual simulation.

Chapter 1

Induction theory

In this introduction, through the classical theory of induction heating is shortly presented.
The main principles, on which the induction heating process is based, are:

- the production of heat is made with eddy currents introduced in the material through electromagnetic induction (Maxwell laws) after being subject under alternating magnetic field;
- the eddy currents, also known as Foucault, creates losses with Joule effect directly inside the material, those are the sources of heating necessary to increase the temperature inside the load;
- the distribution of the eddy currents and the heat sources, is always uneven due to the skin effect;
- the increase of the temperature inside the material is determined through the thermal conduction (Fourier equations).

1.1 Electromagnetic theory

All the following considerations are done on a magnetic steel billet, this means that during the heating not only the resistivity is changing but also the values of the permeability: $\mu = \mu(H, \vartheta)$.
Inside magnetic steel the resistivity is changing in non-linear way: it is increasing 5 times from 0°C to 800°C, while at higher temperature it is slowing down to values that are 7 times bigger than at ambient temperature.
At the same time the permeability at 20°C (μ_{20}) is not only changing with the intensity of the magnetic field, but also with the quantity of carbon in the steel. Because of the high field intensity in these applications, the next equations can be used for the description of the permeability:

$$\begin{cases} \mu = 1 + \frac{B_S}{H_0} \approx 1 + \frac{14000 \div 16000}{H_0} \\ \mu \approx 8{,}130 H_0^{-0{,}894} \end{cases} \tag{1.01}$$

Initially the permeability is changing slowly with the temperature until 500-600°C, after these values it falls to the unit value when the Curie temperature is reached (750-800°C).
The intensity of the magnetic field is going along the billet's axis (z) and intensity similar to the inductor without load:

$$H_0 = \frac{NI}{l} \tag{1.02}$$

with *N* is represented the number of coils, *l* is the length of the inductor [m] and *I* is the value of current inside the coils [A].
Ignoring the displacement current and having for hypothesis sinusoidal values, the Maxwell equations become:

$$\begin{cases} rot\bar{H} = \frac{\bar{E}}{\rho} \\ rot\bar{E} = -j\omega\mu\mu_0\bar{H} \end{cases} \quad (1.03)$$

Where *H* and *E* are the intensity of the magnetic field [A/m]and of the electric field [V/m]; while $j=\sqrt{-1}$.
Because of the geometry of the load-inductor system, only few components of the equations are different than zero, than:

$$\begin{cases} [rot\overline{H}]_\varphi = -\frac{\partial \dot{H}_z}{\partial r} = \frac{\dot{E}_\varphi}{\rho} \\ [rot\overline{E}]_z = \frac{\partial \dot{E}_z}{\partial r} + \frac{\dot{E}_\varphi}{r} = -j\omega\mu\mu_0\bar{H}_\varphi \end{cases} \quad (1.04)$$

Applying to these equations the Bessel function[1]it is possible to obtain similar equations that have adimensional function inside.

$$\begin{cases} \dot{H} = \dot{H}_0 \frac{ber(m\xi)+jbei(m\xi)}{ber(m)+bei(m)} \\ \left|\frac{\dot{H}}{\dot{H}_0}\right| = \sqrt{\frac{ber^2(m\xi)+bei^2(m\xi)}{ber^2(m)+bei^2(m)}} \end{cases} \quad (1.05)$$

It is possible to recreate the effect of the inducted current in function to the adimensional value of the radius ($\xi = {}^{r}/_{R}$).
The *m* is another adimensional value defined as $m = {}^{\sqrt{2}R}/_{\delta}$ and depends:

- proportionally to the frequency (*f*);
- depends on the radius (usually it is constant);
- δ also known as the depth of the skin effect[2], represented in a simplify formula $\delta = 503\sqrt{{}^{\rho}/_{\mu f}}$.

Usually during heating the frequency applied is constant, because of the magnetic nature of the load (steel billet), there is a modification in its electrical proprieties (as stated previously), this means that the *m* is starting with a high value (usually higher than 20) and after the Curie point it becomes lower than 7.

[1] Cylindrical harmonics used in mathematic analysis especially used in signal processing;
[2] Is the tendency of alternating electric current (AC) to become more concentrated along the surface of the conductor.

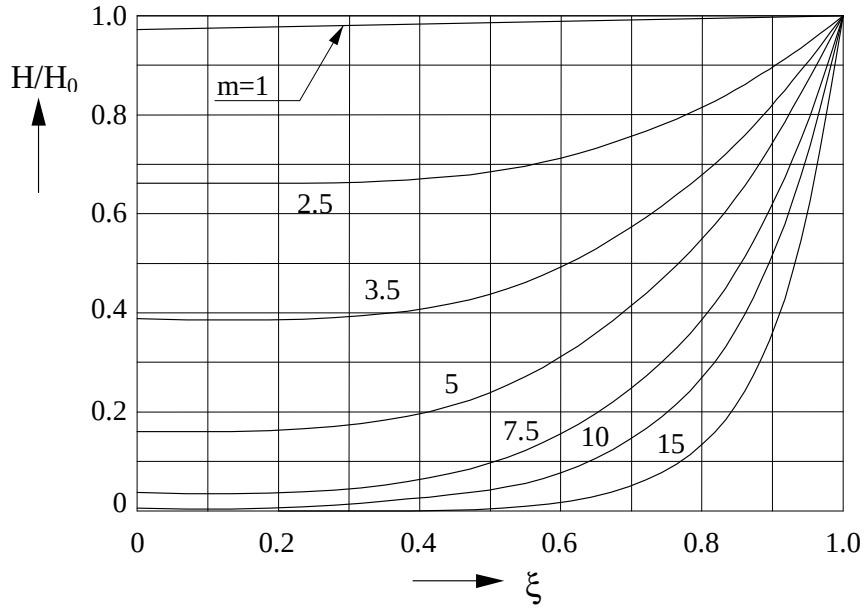

Figure 1.1. *Distribution of the intensity magnetic field H along the radius, reported to the surface value H_0*

It is possible to have similar functions and figure for the density of the current, because$\dot{G} = \dot{E}/\rho$, this means that the Bessel equations will become:

(1.06)
$$\begin{cases} \frac{\dot{G}}{\dot{G}_0} = \frac{ber'(m\xi)+jbei'(m\xi)}{ber(m)+bei(m)} \\ \left|\frac{\dot{G}}{\dot{G}_0}\right| = \sqrt{\frac{ber'^2(m\xi)+bei'^2(m\xi)}{ber'^2(m)+bei'^2(m)}} \end{cases}$$

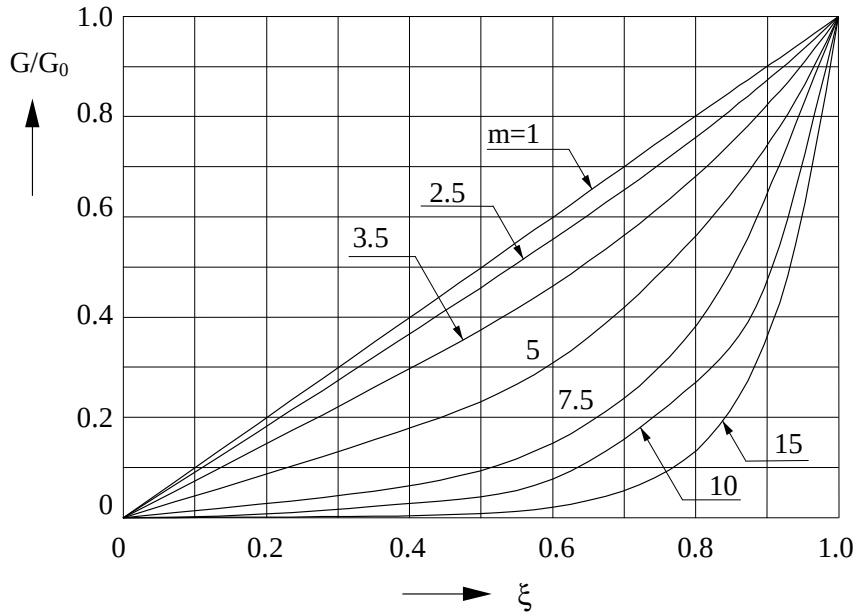

Figure 1.2. *Distribution of the current density G along the radius, reported to the surface value G_0*

Figures [1.1] and [1.2] describe how the magnetic field and the current density are distributed along the radius of the cylinder during the heating, due to the variations of the m. In the beginning when m>15 the depth of the skin effect is few millimetres from the surface, so the majority of the heating source is concentrated inside this distance.

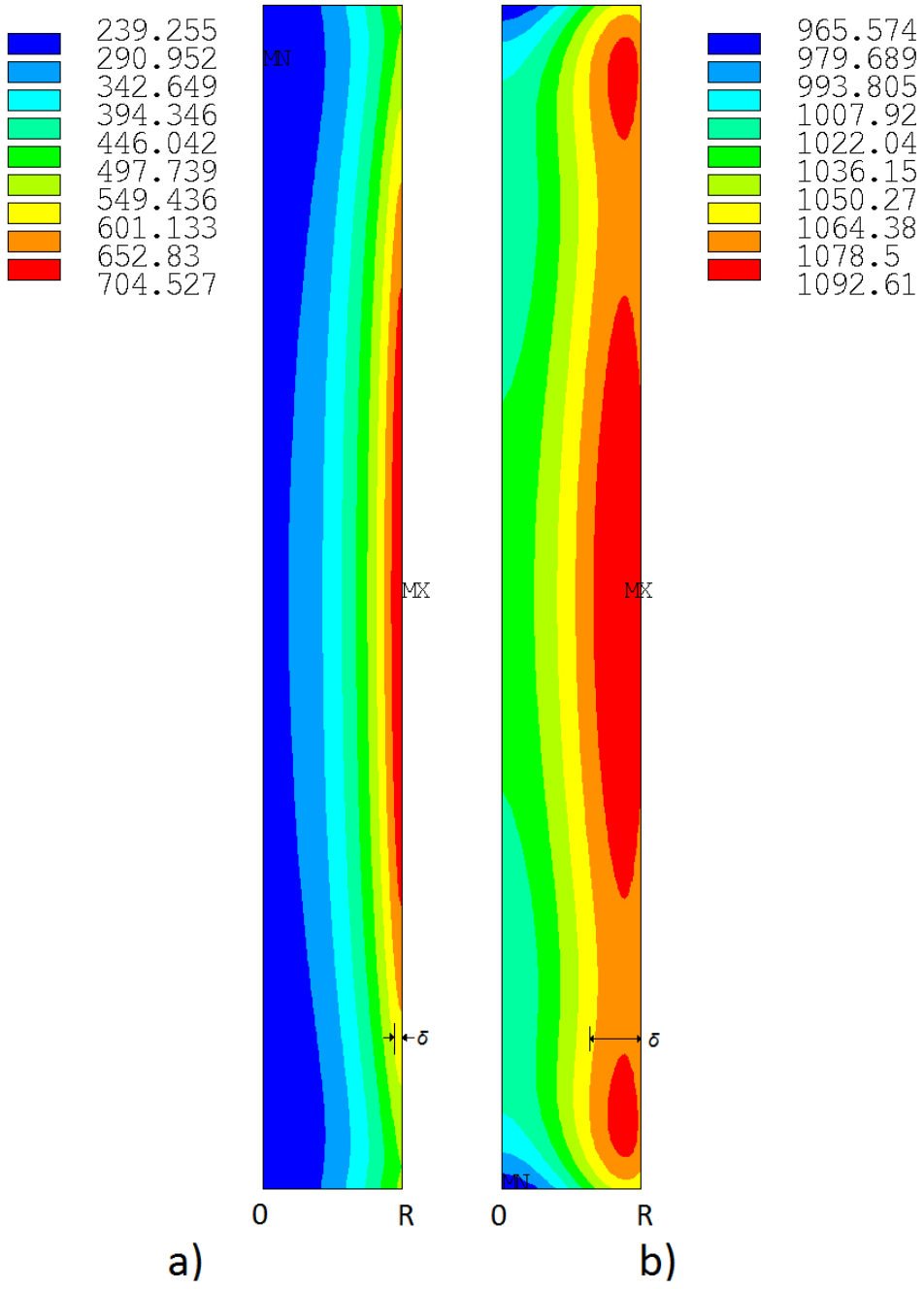

Figure 1.3. *Simulations of a half cross section of a billet before (a) and after (b) Curie point*

Figure[1.3] shows what is happening inside the billet before (a) and after (b) the Curie point. At the beginning of the process the skin effect has a very small depth (δ_a=2,06mm), this means that in the core (r=0) is increasing slowly its temperature only through the thermal conductivity of the material, this explains why the temperature difference between the surface and core is big.

Keeping in mind the considerations above and taking into account the average values of resistivity during the heating, it is possible to estimate the best frequency for various diameter to design an economical process. For uniform heating (see page 10) is conventional to have frequencies usually lower than ten thousand Hertz.

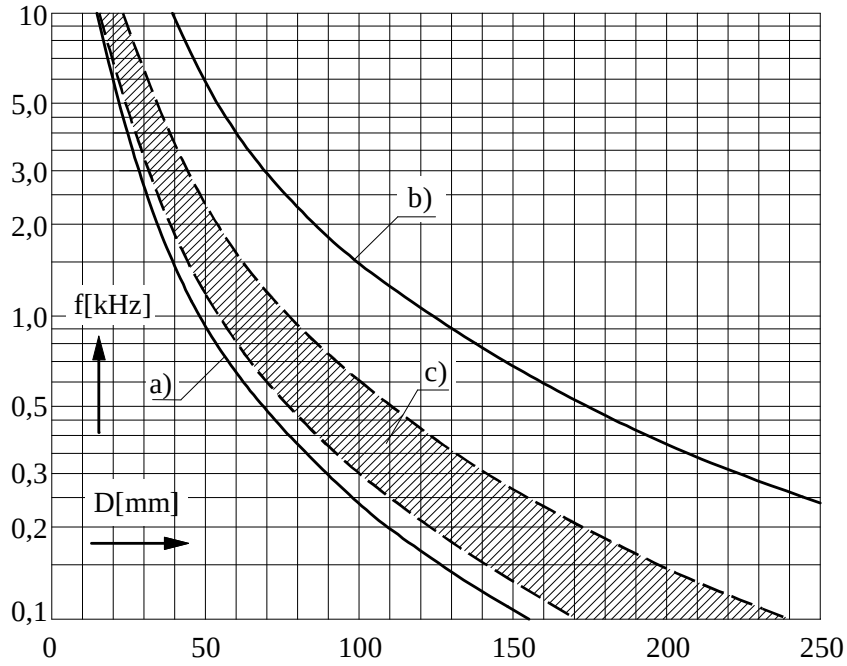

Figure 1.4. *Economical limits for frequency usage in function of the diameter for the heating of steel billets*

From figure[1.4] it is possible to obtain the optimal frequency depending on the diameter of the billet. Lines a) and b) are the upper and lower values of frequency for the heating of magnetic steel from the ambient temperature to 1200°C while the c) are the optimum frequencies that can be measured using a simple formula:

(1.07) $$\frac{3}{D^2} < f < \frac{6}{D^2}$$

In which D is the diameter of the billet (expressed in meters).

The frequency value during heating must also consider m, because:

- m lower than 2,0 means low electrical efficiency (see page 8);
- m equal to 2,5 means optimal frequency;
- m between 2 and 5 means a good heating process;
- m higher than 7 means a low thermal efficiency.

Example 1.1 The diameter of the billet is 65mm, the best values for the frequency are between 755Hz and 1511Hz.

If for example the working frequency is 2000Hz, still inside the range of lines a) and b) (figure[1.4]), and considering the material proprieties before and after the Curie point, it is possible to know how is changing the m value during the process:

- ~700°C m>20
- ~900°C m=3,698

When the m becomes lower than 2 the electrical efficiency starts to decrease (figure[1.5]).

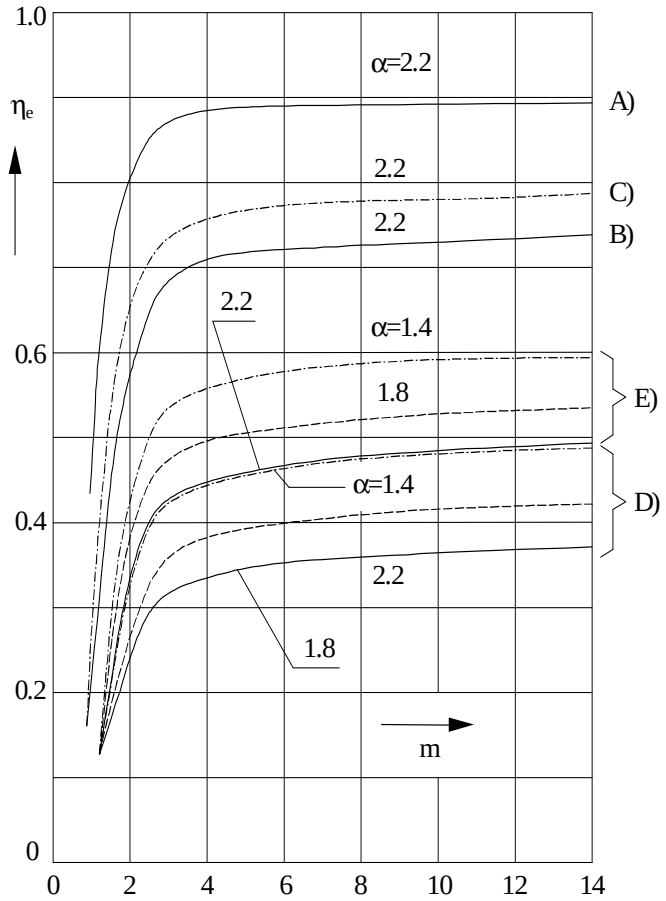

Figure 1.5. *Electrical efficiency of the load-inductor system in function of m: [A-Steel until 800°C; B-Steel from 800°C to 1200°C; C-Steel from 0°C to 1200°C; D-Aluminium and alloys up to 500°C; E-Brass up to 800°C]*

The electrical efficiency (inductor-load system):

$$\eta_e = \frac{r_c' I}{(r_i + r_c')I} = \frac{1}{1+\alpha\frac{l}{l_i}\sqrt{\frac{\rho_i}{\rho\mu}}\frac{A_i k_i}{\sqrt{2}P}} \qquad (1.08)$$

α - is the ratio between the internal radius of the inductor (R_i) and the diameter of the heated body (R);
ρ - and ρi are the relative resistivity of the body and the inductor;
μ - is the permeability of the material;
$A_i k_i$ - is a characteristic of the coil;
P -is a function dependent on the ratio between the m and the dimensions of the body and δ.

The equation (1.08) shows how electric (ρ) and geometric (α) parameters influence the efficiency. Materials with high values of relative resistivity have efficiency values around 0,7÷0,9 while with low values around 0,4÷0,6.

With big values of α the efficiency trend falls, that means that α should not be too high.

The global electrical efficiency during the heating of magnetic steel is based on the same considerations as seen for the equation (1.08), but it is the product of the efficiencies before and after the Curie point:

(1.09) $$\eta_e = \frac{\eta_A t_A + \eta_B t_B}{t_A + t_B}$$

where η_A and t_A are respectively the efficiency and the duration from the ambient temperature to the Curie temperature, while η_B and t_B are after the Curie point to the final temperature. Usually this global electric efficiency has a range of 0,75÷0,8 as seen in the figure[1.5].

The geometric value (α) is also very important in the determination of the power factor.

If the power factor becomes too low, a certain amount of capacitors must be put to prevent problems on the supply line.

(1.10) $$cos\phi = \frac{r_i + r_c'}{\sqrt{(r_i + r_c')^2 + (x_{i0} + \Delta x)^2}} = \frac{1}{\sqrt{1 + \left[\frac{\alpha^2 - (1 - \mu B)}{\mu A}\eta_e\right]^2}}$$

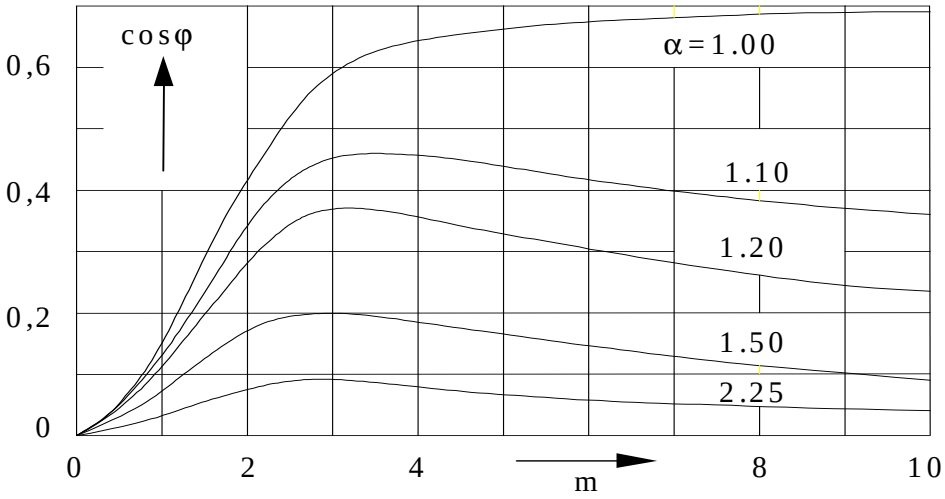

Figure 1.6. *Cosφ values in function of m*

The figure [1.6] shows also how the power factor is changing during the heating and the influence that has the α parameter.

1.2 Thermal theory

The most important thing in induction heating is the determination of the heating times and the power needed so they can be controlled depending on the technological process.
There are two type of heating:

- differential heating, hardening is the most common process
- uniform heating, temperature values are homogeneous through the entire material

All the following considerations are made on the second kind of heating.
Considering a cylinder with a big length compared to the diameter, in which the heating transmission is made in radial direction, and of constant thermal parameters of the material.
The Fourier equation in cylindrical coordinates (r,φ,z) is:

(1.11) $$\frac{\partial \vartheta}{\partial t}=k\left(\frac{\partial^2 \vartheta}{\partial r^2}+\frac{1}{r}\frac{\partial \vartheta}{\partial r}\right)+\frac{w(r)}{c\gamma}$$

ϑ - temperature [°C] along the radius after a certain time t [s] from the beginning of the heating
$k=\lambda/c\gamma$ - thermal diffusivity of the material [m^2/s] – (λ- thermal conductivity [w/m°C], c- specific heat [Ws/ks°C] and γ- density [kg/m^3])
w(r) - specific power per volume transformed in heat [W/m^3]

In the hypothesis that the initial temperature is zero in every point of the cylinder and with heat losses also equal to zero, equation (1.11) can be written with the next initial conditions:

(1.12) $$\begin{cases}\vartheta(r)=0 & for\ t=0\\ \frac{\partial \vartheta}{\partial r}=0 & for\ t>0\ and\ r=R\end{cases}$$

Introducing the next parameters:

$$\xi=\frac{r}{R} \qquad \tau=\frac{kt}{R^2} \qquad \Theta=\frac{2\pi\lambda}{P_u}\vartheta$$

$P_u=2\pi\int_{r=0}^{r=R} rw(r)dr=2\pi R^2\int_{\xi=0}^{\xi=1} w(\xi)d\xi$ -power transformed in heat [W/m]

$$\Psi(\xi)=\frac{2\pi R^2}{P_u}w(r)=\frac{w(\xi)}{\int_0^1 \xi w(\xi)d\xi}$$

The Fourier equation, the boundary conditions and the initial conditions can be written as:

(1.13) $$\frac{\partial \Theta}{\partial \tau}=\frac{\partial^2 \Theta}{\partial \xi^2}+\frac{1}{\xi}\frac{\partial \Theta}{\partial \xi}+\Psi(\xi)$$

(1.14) $$\begin{cases}\Theta(\xi)=0 & for\ \tau=0\\ \frac{\partial \Theta}{\partial \xi}=0 & for\ \tau>0\ and\ \xi=1\end{cases}$$

A linear increase of temperature with the same speed in every point of the cylinder can happen when:

$$\pi r^2 c\gamma \frac{\partial \vartheta}{\partial t} = 2\pi r\lambda \frac{\partial \vartheta}{\partial r} + \int_0^r 2\pi r w(r) dr \quad (1.15)$$

This is an expression of the power needed to increase the temperature of a generic cylinder with radius r with a constant speed ($\partial\vartheta/\partial t$) and the sum of transferred power through the surface with the power transformed in heat inside the cylinder.
Replacing the values with (ξ,τ,Θ), equation 1.16 becomes:

$$\frac{\partial \Theta}{\partial \tau} = \frac{4\pi R^2}{P_u \xi^2} \int_0^\xi \xi w(\xi) d\xi + \frac{2}{\xi} \frac{\partial \Theta}{\partial \xi} \quad (1.16)$$

Developing the equation with adimensional parameters and Bessel functions, it is possible to obtain equations that describe the differences in temperature along the radius.

$$\frac{\partial \Theta}{\partial \xi} = \xi - \frac{ber(m\xi)ber'(m\xi) + bei(m\xi)bei'(m\xi)}{berm\, ber'm + beimbei'm} \quad (1.17)$$

Integrating can be obtained:

$$\Theta = \frac{1}{2}\xi^2 - \frac{ber^2(m\xi) + bei^2(m\xi)}{2m(berm\, ber'm + beim\, bei'm)} + C \quad (1.18)$$

It is possible to define Θ_a which is the value of Θ when ξ=0, this corresponds to the temperature on the axis. While the constant C can be determined with:

$\Theta=\Theta_a$ with ξ=0

and after few steps:

$$\Theta = \Theta a + \frac{1}{2}\left[\xi^2 - \frac{ber^2(m\xi) + bei^2(m\xi) - 1}{m(berm\, ber'm + beim\, bei'm)}\right] \quad (1.19)$$

This equation can calculate the distribution of the temperature along the radius in function of the temperature of the axis.
For $m \to \infty$ the temperature distribution will be:

$$\Theta - \Theta_a = \frac{1}{2}\xi^2$$

this means that for ξ=1 the temperature will be equal to the value on surface ($\Theta = \Theta_s$), the maximal difference between surface and axis can be 0,5.

$$\Theta_s - \Theta_a = \frac{1}{2}$$

If *m* is lower, than the previous equation will have a lower solution that is in function of F(m).

(1.20) $$\Theta_s - \Theta_a = \frac{1}{2}F(m)$$

The function F(m) is considered as a correction factor because in the induction heating the power becomes heat inside the cylinder instead like in surface heating.

(1.21) $$F(m) = 1 - \frac{ber^2 m + bei^2 - 1}{m(berm\ beir'm + beim\ bei'm)}$$

For uniform heating processes it is good to take the average temperature of the cylinder for the calculation of the time, this means that other two functions can be introduced:

(1.22) $$F'(m) = \frac{1}{4} - \frac{berm\ bei'm - beim\ ber'm - m/2}{m^2(berm\ ber'm + beim\ bei'm)}$$

(1.23) $$F''(m) = 1 - 2\frac{F'(m)}{F(m)}$$

With these corrective values it is possible to write the equations for the determination of the time and power needed for heating.

(1.24) $$\begin{cases} t = R^2 \frac{F(m)}{4k\varepsilon}[1 - \varepsilon F"(m)] = R^2 \frac{\pi c\gamma}{P_u}\vartheta_s[1 - \varepsilon F"(m)] \\ P_u = \frac{4\pi\lambda}{F(m)}(\vartheta_s - \vartheta_a) = 4\pi\lambda\frac{\varepsilon}{F(m)}\vartheta_s \end{cases} \qquad \varepsilon = \frac{\vartheta_s - \vartheta_a}{\vartheta_s}$$

Where:

- ϑ_s is the temperature on the surface;
- ϑ_a is the temperature on the axis.

Equation (1.24) describes the influence of the ε and frequency used on the time of heating and the power needed:

- increasing the frequency means that F(m) becomes bigger and we would have a lower value of power and a higher time;
- for low ε (maintaining same frequency) the power goes down and more time is needed;
- if ϑ_s and time are assigned, than the power can be easily found and the only way to reduce the ε is by choosing the right frequency value;
- if ϑ_s and ε are given, than it is possible to rise the power so the time becomes shorter.

In these observations the radiation and convention losses on the surface were not considered. These losses on one side reduce the power needed for the temperature increase, so the heating time would

rise, and on the other side the difference of temperature between the surface and the core would decrease.

But because the billet is made of magnetic steel, this means that the process is non linear because the material proprieties are different before and after the Curie point.

It is possible to divide the heating in two phases: A before the Curie point and B after it and in both the P_u is constant.

From the equations (1.24) it is possible to obtain:

$$\frac{m_B}{m_A} = \sqrt{\frac{f_B}{f_A}}\sqrt{\frac{\rho_A}{\rho_B \mu_A}} \tag{1.25}$$

$$\frac{P_{uB}}{P_{uA}} \approx \left(\frac{H_{0B}}{H_{0A}}\right)^2 \sqrt{\frac{f_B}{f_A}}\sqrt{\frac{\rho_B}{\rho_A \mu_A}}\left(\frac{P_B}{P_A}\right)\frac{1}{1{,}37}$$

Using the average temperature of the billet during the heating, it is possible not to consider the εF"(m) paramete.

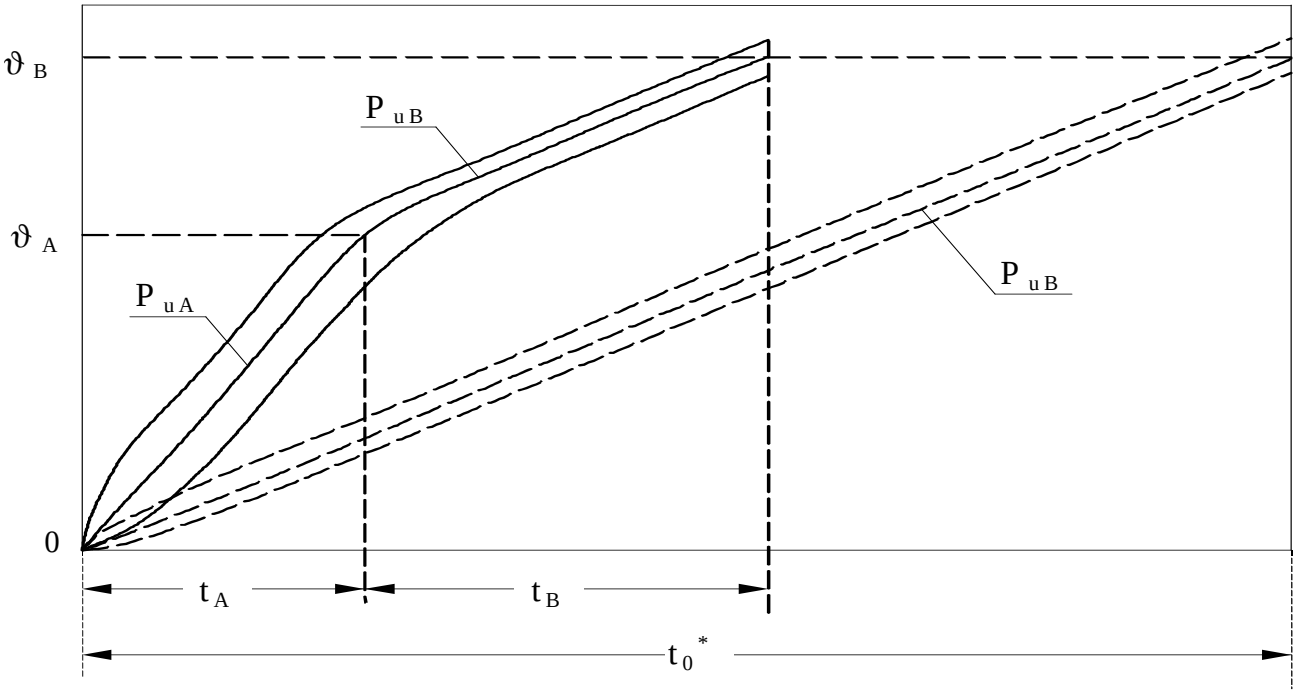

Figure 1.7. *Schematization of the thermal transient for the approximation of heating time for magnetic steel*

The total time for heating a magnetic billet is:

$$t_0 = t_A + t_B \approx \pi R^2 \left[\frac{c_A \vartheta_A}{P_{uA}} + \frac{c_B(\vartheta_B - \vartheta_A)}{P_{uB}}\right] \tag{1.26}$$

If it is considered an ideal heating where is used the P_{uB} during the entire process, than the time needed would be t_0^* and it is possible to have the next equations:

$$\frac{t_0}{t_0^*} = \frac{t_A + t_B}{t_0^*} \approx \frac{\vartheta_A \frac{P_{uB}}{P_{uA}} + (\vartheta_B - \vartheta_A)}{\vartheta_B}$$

(1.27)

$$\frac{t_A}{t_B} \approx \frac{\vartheta_A}{\vartheta_B - \vartheta_A} \frac{P_{uB}}{P_{uA}}$$

(1.28) $\frac{t_A}{t_B} \approx 0{,}2 \div 0{,}36$ $\frac{t_0}{t_0^*} \approx 0{,}47 \div 0{,}53$

For inductors in which the coils have the same gap:
m is always above 25 if the heating is under the Curie point (t_A)
the power necessary to heat is usually lower after the Curie point (t_B)
As shown previously with the equations (1.25) and (1.27), a reduction of those times can be obtained by changing the ratio (P_{uB}/P_{uA}) using inductors with different coils, which will change the ratio (H_{0B}/H_{0A}). This reduction can be done by changing the frequency in the inductor that is heating previously the Curie point.
Another method to reduce the heating time is with "fast" heating. This method uses higher value of power so the surface reaches the maximum temperature in a very short time. In this first moments the $\Delta\vartheta = \vartheta_s - \vartheta_a$ is very high, but after, the heating is done with lower power so the temperature on the surface is constant and the ε reaches the final desiderated value.

Example 1.2 - Considering the proprieties and the dimensions of the billet (Ø=65mm, L=273mm), it is possible to make some estimations on the duration needed to heat a magnetic steel billet. The variables are selected from the material proprieties depending on the temperature.

For T_{sA}=757°C: *λ=41 W/m°C c= 624 W/kg°C ε=0,57 m=29,8*
For T_{sB}=964°C: *λ=26,4 W/m°C c= 655 W/kg°C ε=0,084 m=3,798*

It is possible to obtain the time when reaching the Curie point
t_A = 36s t_0 =153s
t_B =117s t^*_0 =342s

The ratios of these values are almost within the range of the theory (equations (1.28)), in fact they are:

$$\frac{t_A}{t_B} = 0{,}31 \qquad \frac{t_0}{t_0^*} = 0{,}45$$

Chapter 2

Outlook of forging industry in European

In 2009 final energy consumption in Europe was around 1155Mtoe (lower than in 2008 because of the economic crisis) and it is only the 14% of the total 8353Mtoe consumed in the world.
This Final Energy[2.1] was used in different sectors:

- Transport 365Mtoe
- Households 307Mtoe
- Industry 292Mtoe
- Service 152Mtoe
- Agriculture 25Mtoe
- Fishing 1Mtoe
- Other 11Mtoe

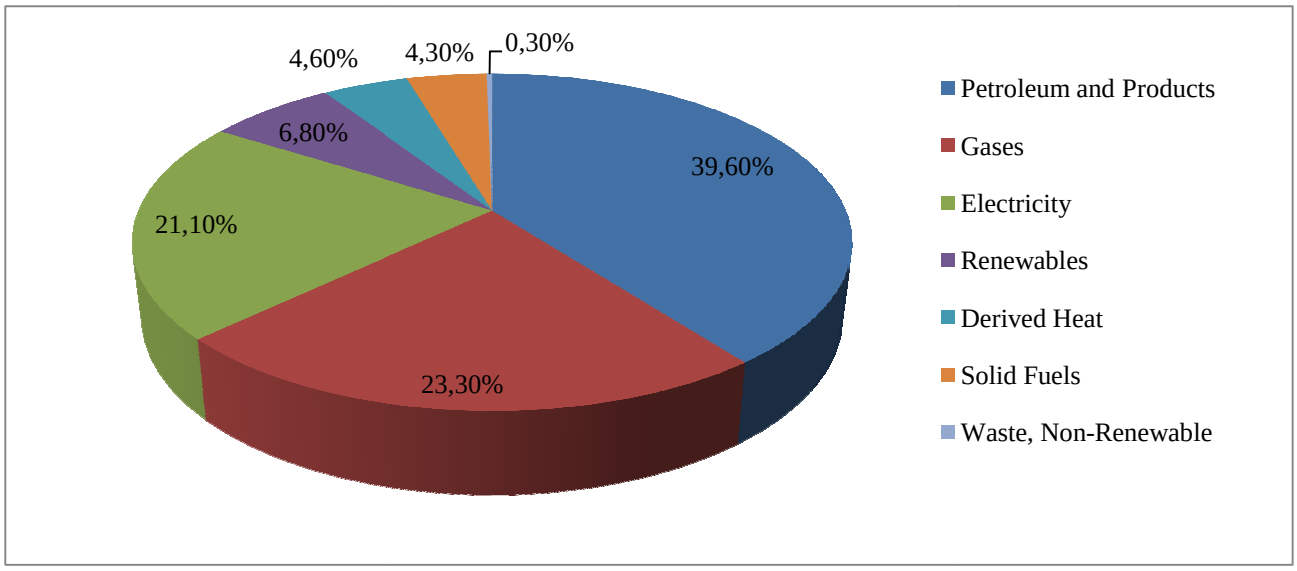

Figure2.1. *EU-27 final energy consumption*

The industrial consumption is the third on the previous list and in the next graph we see the share of final energy for different sectors (from 2000 to 2007)[2.2].

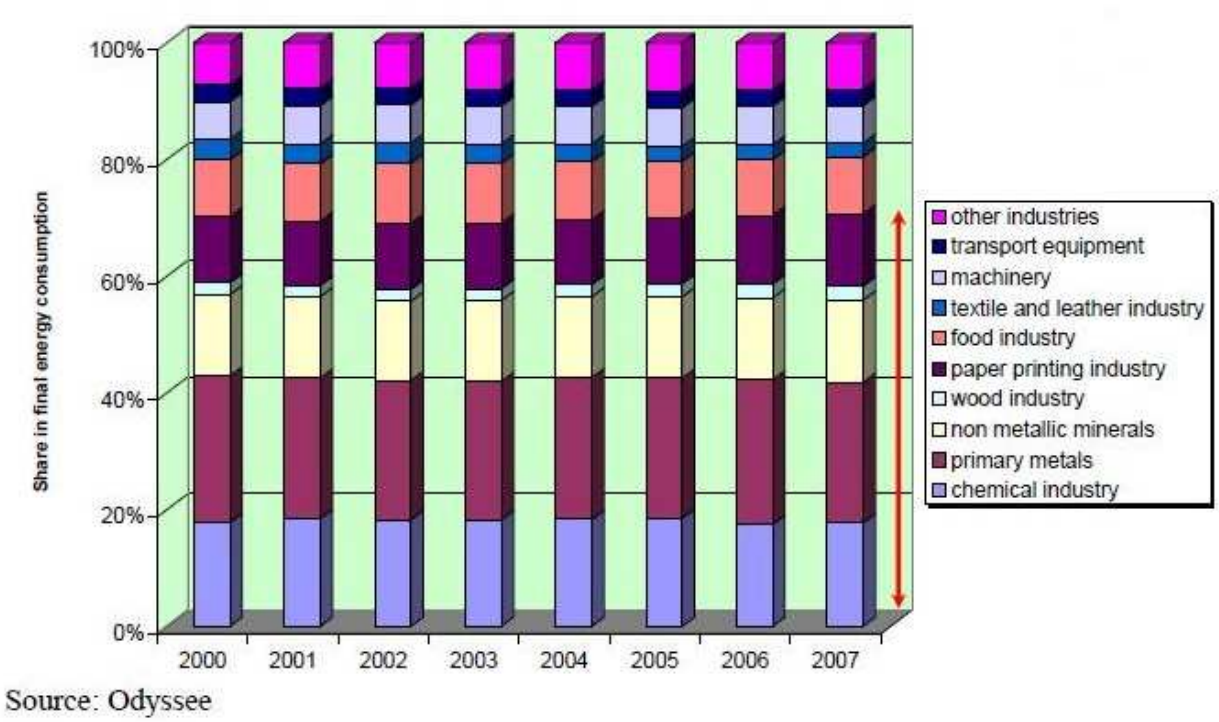

Figure2.2. *Final energy for different sectors*

The European Union spent 3,133,762GWh in 2009 and this is the sum of all the 12 the industrial sectors (iron & steel industry, non-ferrous metal industry, chemical industry, glass, potter & building material industry, ore-extraction industry, food, drink & tobacco industry, textile, leather & clothing industry, paper and printing, transport equipment, machinery, wood production, construction).

The forging sector is part of the Iron & Steel industry in which, only in 2009, were spent more than 514TWh[(2.3)] and most of the energy came from coal and gases.

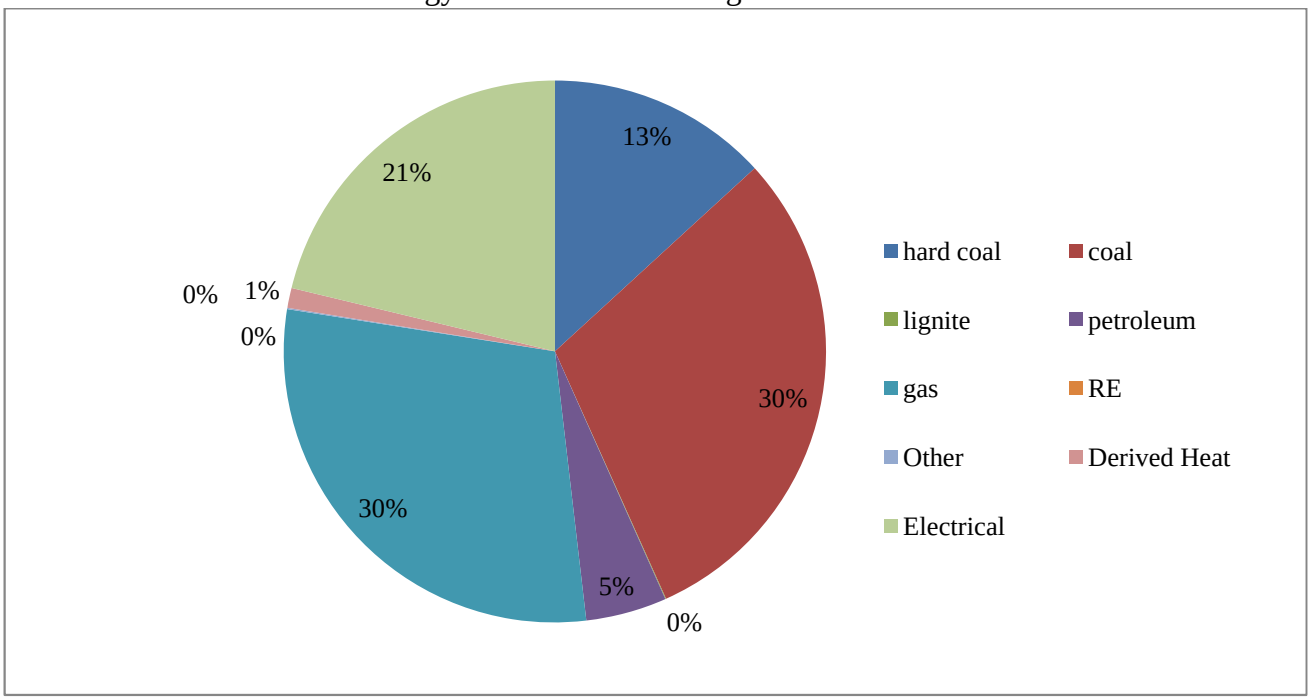

Figure2.3. *Energy used for Iron & Steel Industry EU-27 2009 (total 514344 GWh)*

In the EU15 electricity consumption rapidly increased until 2000 (1.7%/year in the period 1990-2000) with a net slow down thereafter (0.9 %/year in the period 2000-2007). This fast increase was partly due to structural changes towards more electricity-intensive sectors (i.e. equipment manufacturing) and additional substitution. In the new EU12 countries, this was different due to the structural changes and electricity savings in the nineties (-3.7 %/year decrease in electricity consumption in 1990-2000) with an economic rebound after 2000 (+2.5 %/year in the period 2000-2007). As a result, electricity consumption in the EU27 grew at a somewhat higher rate in 2000-2007 (1.05 %/year), but the reason that triggered further growth was mainly based in the rebound effect of the new Member States.

Of the 21% of electricity used in the iron & steel industry, 80% is used for the alimentation of motors and process technology. In this last part is also included the electrical energy used in an induction heating process.

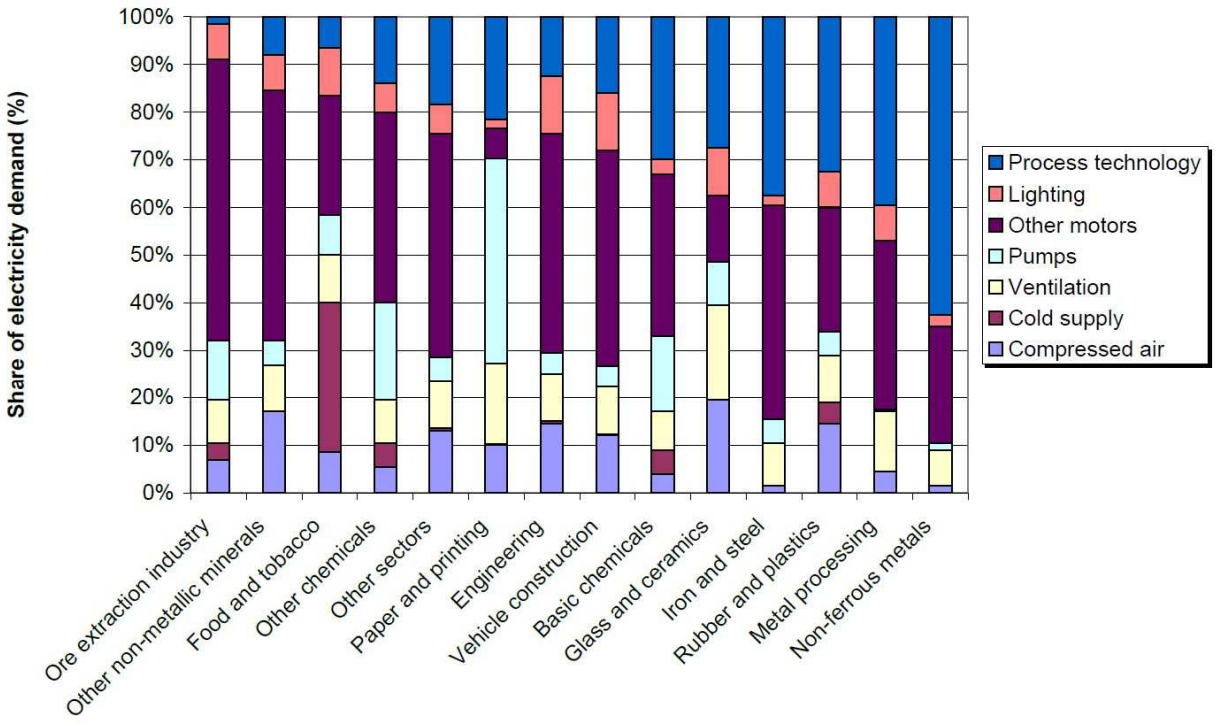

Source: Fraunhofer ISI

Figure2.4. *Share of energy-intensive sectors in final energy consumption*[(2.2)]

2.1 Forging overlook in the EU

The EU-27's forging, metal coating and mechanical engineering sector was the largest in terms of enterprise numbers, persons employed and EUR 60.2 billion of added value in 2006, about one quarter (24.6 %) of the total value added for metals and metal products manufacturing. About three quarters (72.2 %) of the EU27's value added in the forging, metal coating and mechanical engineering sector in 2006 came from the treatment and coating of metal and general mechanical engineering subsector, the remaining share coming from the forging, pressing, stamping and roll forming of metal subsector. Germany made the largest contribution (23.7 %) to the value added created by the forging, metal coating and mechanical engineering sector across the EU27 in 2006. It was only a little more than the contribution from Italy (22.1 %), the most specialised Member State in forging, metal coating and mechanical engineering, where these activities contributed 2.1 % of non-financial business economy value added in 2006, which was almost double the EU27 average.

Table 2.1. *Production of EUROFORGE members in 2011*[2,4]

Total production of forgings (metric net tons x 1000)	Germany	Italy	France	Spain	United Kingdom	Belgium	Sweden	Czech Republic	Poland	Slovenia	Finland	EUROFORGE member
Close die forge, press upset forging	2137	815	299	262	179	0	89	121	180	35	9	**4091**
Cold forging	299	0	41	18	26	11	0	19	0	6	1	**421**
Open die forging	399	425	45	76	25	0	0	170	115	0	0	**1255**
Closed die forging of non ferrous metal	56	0	10	0	5	2	0	12	0	0	0	**85**
Total Production of the year	2891	1240	395	356	235	13	89	321	295	41	10	**5886**

2.2 Forging in Germany

From the EuroForge annual member analysis (table[2.1]) it can be seen that Germany has the biggest share in the forging sector. Almost half (49%) of the forging production comes from Germany and second biggest contribution comes from Italy with 21%, but has the biggest production of open-die forging (425kton in 2011).Germany's drop-forging sector is leading in Europe (followed by Italy), but on a world-wide production it is still the second because of the economic grow in China. The production can be seen in figure[2.5] until 2008.

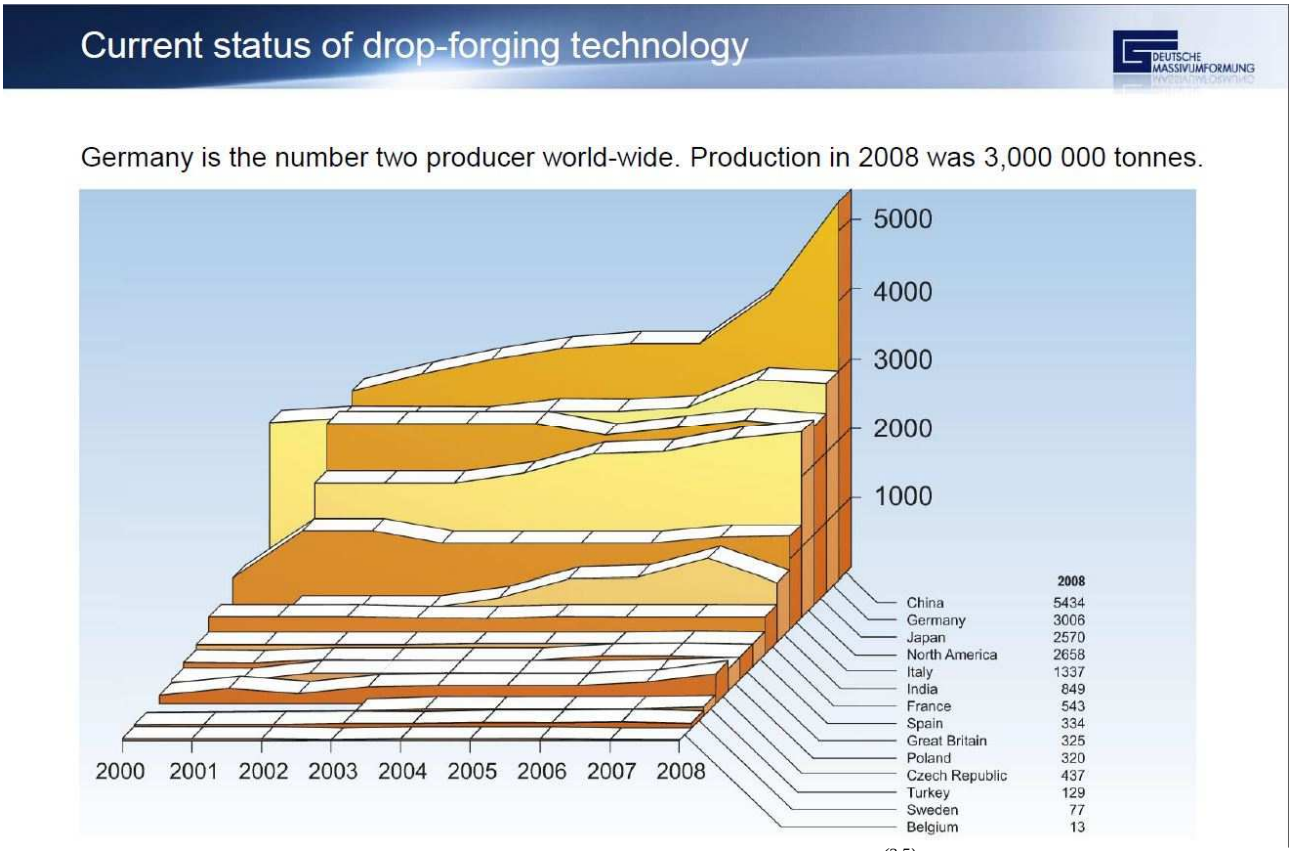

Figure2.5. *World drop forging production 2008*[2.5]

Germany's production of drop-forging before the crisis (2008) was 3006kton, after it drops to 1280kton (in 2010).

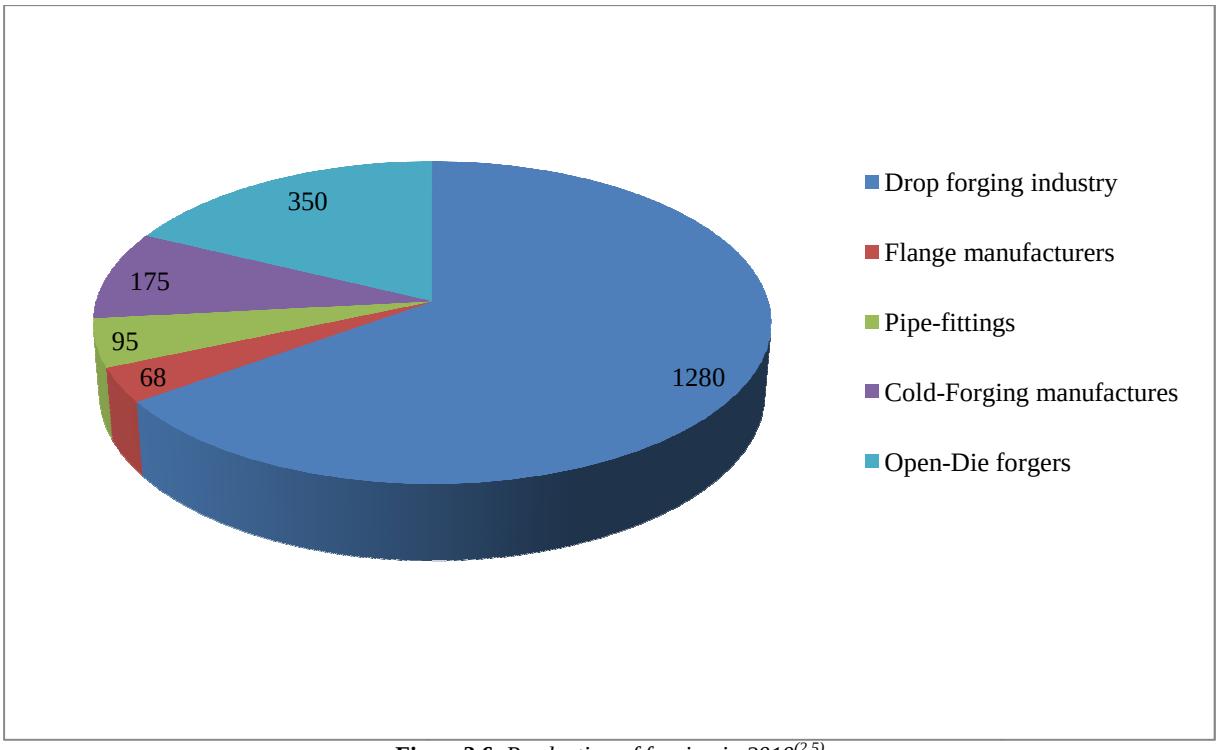

Figure2.6. *Production of forging in 2010*[2.5]

Around 35% of all forged parts in Germany are exported.

The automotive sector, together with system producers (tier one suppliers) receives more than 80% of total production.

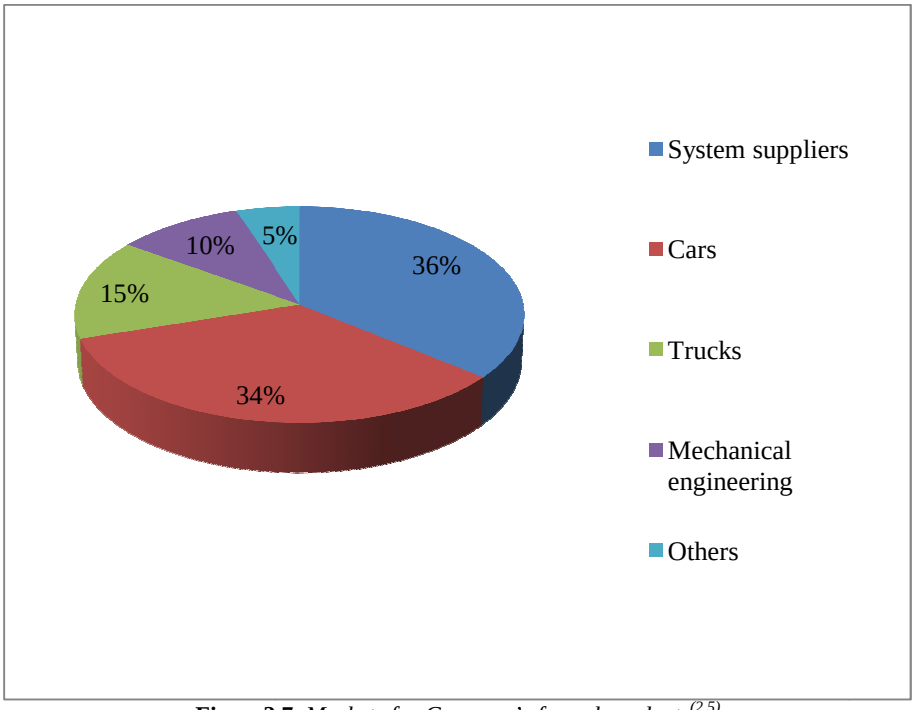

Figure2.7. *Markets for Germany's forged products*[2.5]

Chapter 3

Forgings

Because of the field of application, it is important to have knowledge of some of the treatments in forging industry.

3.1 Forging types

3.1.1 Die Forging

The industrial established forging method is open-die press forming with flash, because precise production and exact positioning seemed long to be too difficult in mass production. The tools for open-die press forming with flash have a geometrically defined flash gap to control pressure in the dies and form filling. During die forging the tools constitute a material flow in tool moving direction and across. This so called guided extrusion consists of three main forming operations: upsetting, rising and spreading. Upsetting is in tool moving direction, rising against and spreading across tool moving direction. The advantages and disadvantages of die forging in comparison to alternative production methods e. g. milling, turning and casting are listed in the following:

- Advantages:
- low cycle time connected with high production rate,
- low material consumption,
- expedient fibre flow
- low machining effort

Disadvantages:

- high costs for equipment, dies and heating

3.1.2 Flashless precision forging

Precision forging is a special technology of flashless forging in closed dies. In contrast to this definition, precision forging in industrial applications is defined by the tolerances with no regard on the flash. Tolerances from IT[3] 7 to IT 9 and in special cases IT 6 can be achieved using precision forging. Work pieces ready for installation can be produced using precision forging. Thus, post-forging machining e. g. milling of the work pieces can be reduced significantly in comparison to common forging with flash, because selected functional surfaces must be machined only. Simple axis symmetric parts (e. g. gear wheels and conical gear wheels) are already produced with functional surfaces ready for installation. In this moment, precision forging is in most cases applied

[3] International Tolerance is a standardised measure of the maximum difference in size between the component and the basic size;

at the production of gear wheels for aircraft industry. Precision forging shortens process chains by eliminating trimming operation[4] and time-consuming machining because of the near-net-shape geometry. Additionally, no deformation of the work piece caused by trimming occurs. The main advantages of precision forging in closed dies are:

- increase of material efficiency,
- no trimming necessary,
- short process chain,
- reduction of machining,
- increase of accuracy grade and
- more precise mass distribution.

For the tool design high reproducibility and high precision (up to two IT-classes closer than the work pieces) are enquired. So these parameters can be considered for tool design. In order to reach this precision high demands have to be met:

- precise tool design and tool manufacturing,
- high volume and geometrical accuracy of the raw material and the work pieces,
- precise guiding of temperature,
- tool and machine guiding in close tolerances,
- high process stability,
- high reproducibility of process parameters and
- define process.

3.1.3 Tool and machine technology

The tool technology for flashless precision forging is different in comparison to tools for conventional die forging. For precision forging closed dies are used to guarantee that no material extends from the dies. This demands a high precision of the raw parts and the material must not be able to flow through the contact zone between upper and lower die. Thus, special closing systems are necessary. The easiest way to close the dies is to use the upper die as a punch which drives into the lower die and forms the complete die impression. This is used e. g. for precision forging of claw-pole rotors. Another possibility for die closing is a system which consists of an upper punch and lower punch (the lower punch can be used as ejector) and floating dies. One further tool technology for flashless precision forging is a system with a hanging closing plate. This system uses one stationary die with one central mounted ejector, one punch and one closing plate. The closing plate surrounds the punch and braces itself from the punch using clips. These described technologies were developed in a first approach for rotational axis symmetric parts e. g. gear wheels.

[4] A shearing operation that removes an uneven section from the top rim of a previously worked part. Trimming operations typically follow drawing operations of sheet metal.

The total mass has to be constant during all forging operations, the pre-forms have to be reproducible and the insertion/positioning in the tools has to be precise. For the precision forging production of long parts the accuracy of the volume distribution plays a more important role than at common forging, because the mass has to be distributed in two directions and not only along the longitudinal axis. The number of pre-forming steps is connected with the shape of the work piece: An increase of geometry complexity increases the number of pre-forming steps.
The tool concept for precision forging of long parts is based on the disconnection of die closing and forming/forging. After the closing of upper and lower die without any forming the upper and lower punches enter the gravure and execute the forming. So, additionally springs are necessary in order to absolve the independent movement of the lower punch. An example of a tool system to forge a typical long part (connecting rod) is given in figure[3.1].

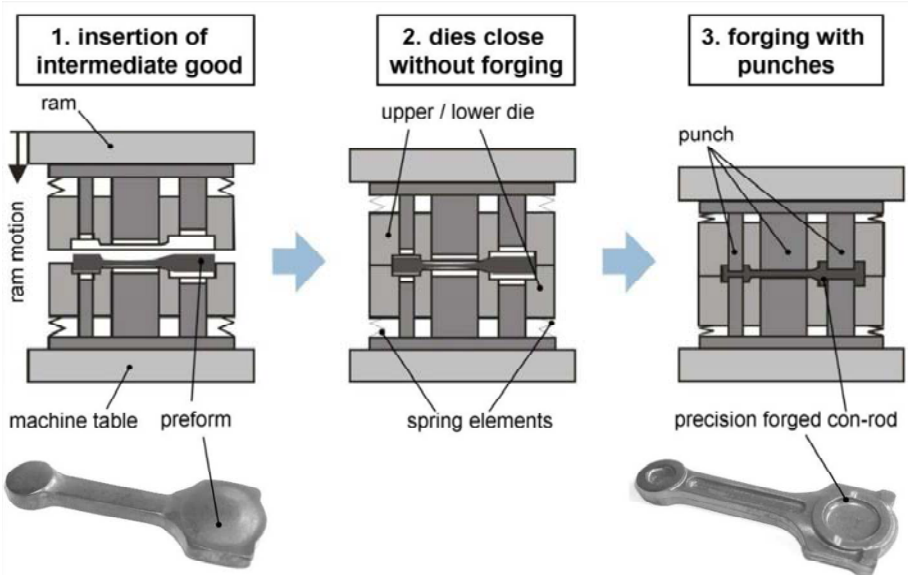

Figure 3.1. *Flashless precision forging of connecting rod (long part)*

This complex tool concept is a result of the need of a relative move between the dies and the punches. This relative move is necessary to achieve the following two functions: First, it realises the force to close the dies and, secondly, it enables the entering of the punches in the dies. Due to this tool design the punch move in the opposite direction can be realised at different speeds. These speeds control themselves according to the principle of constant forming resistance. Furthermore a double acting forming can be realised.

3.1.4 Application of precision forging with steel materials

In combination with a cold calibration, the precision forging is industrially established for the production of conical gear wheels for differential gears.
An innovative forging sequence for flashless forging sequence for crankshafts[5] of a two-cylinder crankshafts was developed for the project SFB 489 by the "Prozesskette zur Herstellung

[5] Complicated high duty forged parts as engine crankshafts are one of the most critical loaded components in engines, enduring cyclic loads as bending and torsion. Since a crankshaft endures a large number of load cycles during its service life, fatigue

präzisionsgeschmiedeter Hochleistungsbauteile" of the German Research Foundation DFG. The forging sequence consists of four stages and was experimentally tested. During the first two stages, the mass of the crank web is allocated by lateral extrusion. The next stage is a multi-directional forging operation to form the cross sectional area of the crank webs. In this phase, the crank web is formed and the crank pin is displaced radial while an upsetting of the part takes place. Finally, the last forging stage creates the near net-shape end geometry without flash. An overview of the developed 4-step forging sequence is given in figure[3.2]. The multi-directional pre-forming is done in the third step.

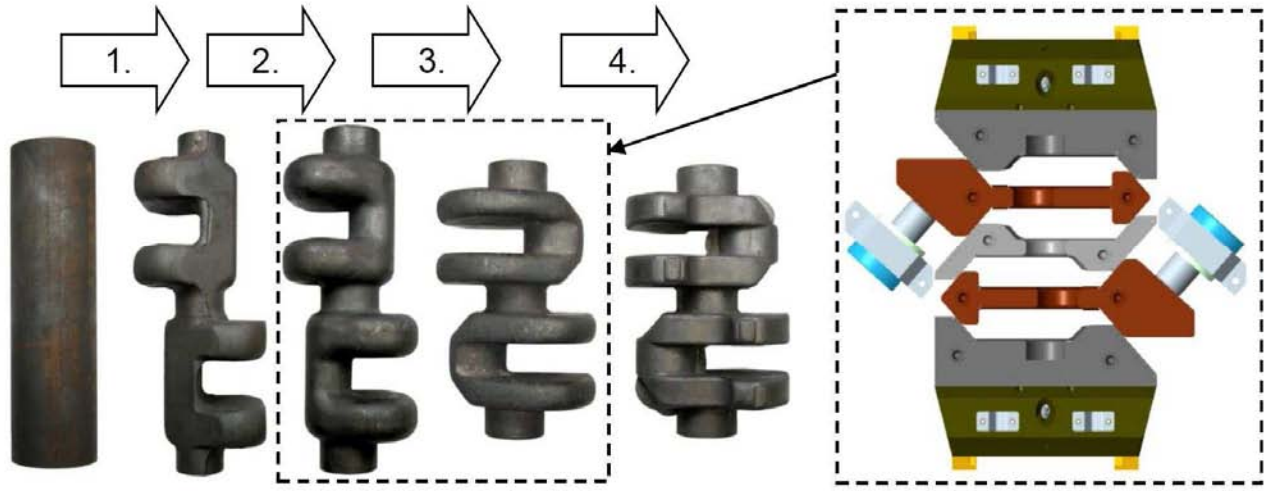

Figure 3.2. *4-Step flashless precision forging sequence of two-cylinder crankshaft and multidirectional preforming tool (SFB489)*

These researches show a possibility of flashless precision forging of crankshafts and its complexness. However, the tool loads (die stresses), tool costs and the design effort are very high. Due to high die stresses, the risk of tool failure is too high and has not been solved. In addition, using a single press for all four forging steps, the needed press force would not compensate the gain from a complete flashless final forging. Therefore an industrial application of this technology is not given until now.

3.1.5 Flash reduced forging technology

The advantage of these technologies is that the mass of the raw part after cutting/before forging is exact the same of the final work piece after forging and no scrap material will occur. Thus, the material utilization is nearly 100 %. The disadvantages are the high effort for tool design, high tool costs and high tool loads in the precision forging step. The tools used in the SFB489 cost around

performance and durability of this component is a key consideration in its design and performance evaluation. High strength, ductility, and fatigue resistance are critical properties required from the crankshaft material and manufacturing process. Fatigue is the primary cause of failure of crankshafts due to the cyclic loading and presence of stress concentrations at the fillets. Other failure sources of crankshafts include oil absence, defective lubrication on journals, high operating oil temperature, misalignments, improper journal bearings or improper clearance between journals and bearings, vibration, high stress concentrations, improper grinding, high surface roughness, and straightening operations.

100 k€, which is quite much in comparison to 50 - 60 k€ for conventional forging tools. High tool load can cause cracks in the tools and too much wear.

The flashless preforming operations and a flash reduced final forming should need virtually equal press forces and therefore be the best way to realise a most efficient process chain. This so called flash reduced forging also aims at a significant flash reduction. The preforming is similar to flashless precision forging including multidirectional forming.

The achievable material utilization is up to 95 % and is an innovative advancement in comparison to conventional forging with flash, which reaches a material utilization between 60 and 80 % only. For flash reduced forging a flash ratio of about 5 % is technically necessary to avoid defects of the crankshaft e. g. folds and cracks: Some material can extend from the final die and pressure in the tools is decreased. The development of a flash reduced forging sequence is almost similar and complex as the development for flashless forging because three of four forming steps are the same and the same lay-out method must be used. Only the last forming step is with flash and improves the industrial application significantly: the forces are much lower, the risk of tool damage is eliminated, variations of raw material mass are compensated and the risk of folds and cracks decreases.

Table 3.1. *Summary of forging methods*

Forging method	**Advantages**	**Disadvantages**
Flashless	Highest material utilization: almost 100 % High precision of forgings	Complicated process High forces 100 % constant raw part mass essential Risk of tool damage/break Very short tool life time High costs / no cost saving
Flash reduced	High material utilization: up to 95 % (significant increase in comparison to conventional forging) Cost saving possible Industrially marketable, especially for SMEs	Multi directional tool necessary Higher tool costs than conventional forging Broken fibre flow
Conventional	Simple process Low tool costs	Low material utilization: 60 to 80 % No significant improvements possible No significant cost/material saving possible Broken fibre flow

From an economic point of view, at flash reduced forging, the cost saving due to material and energy saving is higher than the increase of tool and process costs. At flashless forging the additional costs for the complicated process are much higher than the cost savings and make this technology inappropriate for industrial application. For the conventional forging technology, no significant improvements concerning material utilization and cost savings are possible.
One crankshaft was experimentally flash reduced forged using the SFB489 tools for flashless forging to show the general feasibility. The work piece temperature was around 1250 °C and the material 42CrMo4 was used. All three pre-forming operations were done flashless and at the last forming step a new tool was used allowing flash. But, this crankshaft has a lot of failures like large folds were found and is not usable for industrial application. It is shown together with a conventional and flashless forged crankshaft in figure[3.3].

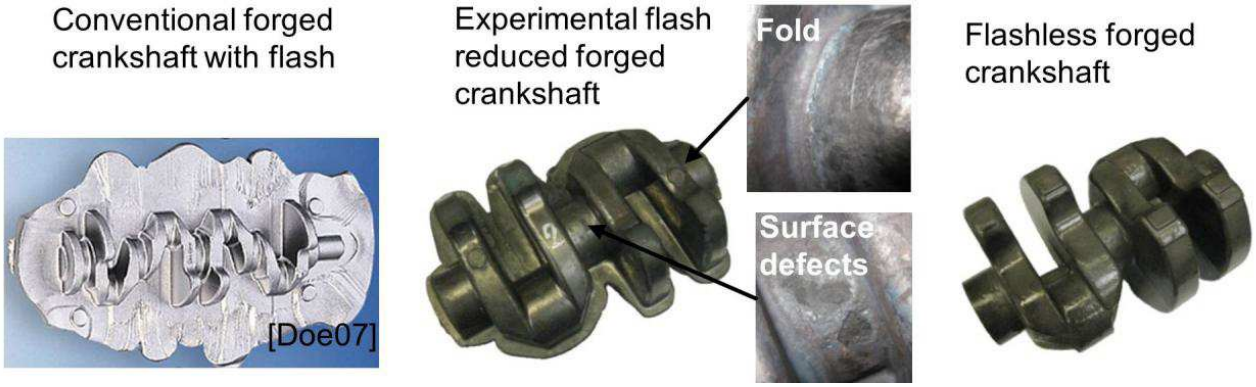

Figure 3.3. *Comparison of crankshaft forging technologies*

Usually, crankshafts are manufactured by casting or forging processes. Forged parts have the advantage of more compact and homogeneous structure, with less micro-structural defects. Selection of the right forging technology (dies design, forging steps and process temperatures) is critical for the mechanical characteristics of the forged crankshaft, as strength toughness and fatigue resistance. The forged structure should be characterised by the grain flow oriented to the principal stress direction. The directional properties resulting from the forging process help the part acquire higher toughness and strength in the grain-flow direction.

3.2 Induction reheating

It is not uncommon for a partially completed forging to be reheated before performing the next forging steps. As the work piece initially heated to the hot working temperature becomes chilled during the forming and transport, a reheating may be necessary prior to further forming operation.
For reheating of irregularly shaped work pieces being processed mainly in drop forges, small-diameter rotary heart furnaces are used today. For large forged parts, which are normally reheated individually or in very small batches, bogie-heart furnaces are preferred. Chamber furnaces may be used for lighter parts and pit furnaces for long cylindrical material. Furnaces based on different heating technologies can be found in the forging industry. However, contrary to the initial heating

prior to forging, the induction heating is not used for reheating of partially completed forging parts at all, as their geometrical properties are mostly inapplicable for reheating in a standard induction furnace, whether it is a static or continuously working installation. For that reason, all available solutions related to reheating by means of induction techniques work with constant cross section along the length of the work piece, e.g. systems for reheating of wrought billets before further manufacturing.

Chapter 4

Potential for saving of energy in forging industry

It is interesting to understand where are the major wastes of energy, so it is possible to intervene for possible savings. Also a look if it concerns only the machinery used or also the type of process, analyzing how this is resolved in the REForCh project.

4.1 Energy consumption

The average energy required for heating one ton of steel is 400 kWh.
The electric energy that comes from the system usually has to go through: the transformer, the converter, the capacitors and the bus bars. This means that before arriving to the inductor, the system would already have a 6% of losses.
Usually in this kind of heating process the temperatures are very high, it is very important to install a water cooling system that can maintain the inductor's temperature lower than the melting point of copper (commonly used for the coils). This means that the thermal losses in the inductor are around 4% the energy needed from the supply line for the heating. While the radiation losses are 2%.
Because the electrical losses are the biggest, around 22,6%, it is very important to use specific inductors with specific diameters, because this can change α and the total electrical efficiency (Chapter 1 – Electromagnetic Theory). The final useful energy, to heat one ton of steel, is 278 kWh, which means an efficiency of 65%.

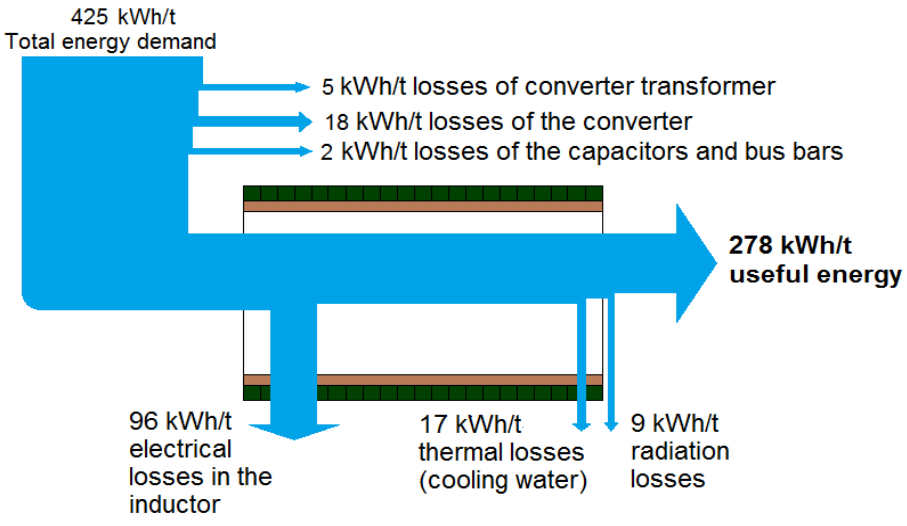

Figure 4.1. *Typical energy flux in an induction heater*[4.2]

Taking in consideration these percentages and the data from the Euroforge members (table [2.1]) it is possible to calculate the total energy consumption during the 2011.
Using the value of 400kWh/t[(4.1)] and remembering that the production was 5886kton, the energy needed from the 586 plants was 2501,5GWh.[6]

4.2 Material Savings

Typically during the forging of parts with flash the material utilization is, depending on the work piece complexity, between 60 to 80% of the raw material. But with flash reduced forging material, utilisation can be increased to over 90% even for the more complicated geometries with a relative high weight ratio.
As an example the weight of a conventional 4-cylinder crankshaft is about 12 kg. Assuming a material utilisation of 75% the initial weight of the billet is 16 kg. An increase of the utilisation up to 90% leads to 2,7 kg less material for each crankshaft (17% less). Since in Europe 15 million cars are produced each year, 40.000 tons of steel can be saved. With a steel price of around 1 €/kg the total amount of about 40 million Euros can be saved just with the material reduction.
The total production of passenger cars, not considering commercial vehicle cars, in Europe was about 15 million in 2010. Due to the low level of electrical cars, almost every car has a crankshaft. A typical crankshaft for a medium sized engine (4 cylinders) has a net weight of about 12 kg and is produced by forging with a material utilization of about 75% which sums up to a gross weight of the forged crankshaft of 16 kg. This means that every crankshaft has about 4 kg of flash. An increase of the material utilization to 90% would decrease the weight of flash to 1.3 kg per crankshaft which is a saving of 2.7 kg. Hence, the savings in material consumption for 15 million crankshafts are about 40,000 tons annually which has a value of more than 40 million € (800 € per ton of steel).
As said previously, the energy required for the production of forgings is mainly caused by the induction heating. Compared to forgings with flash 17% of the heating energy can be saved by the reduced raw material which needs not to be heated. Hence, the scrap production and raw material production for crankshafts can be reduced.
This means that for the European cars industry the saving on energy consumption would be about 1,08 kWh per crankshaft (2,7 kg * 0,4 kWh/kg) and therefore an annual saving of 16,2GWh per year. This energy savings can decrease the European CO2-emission by about 10,000 tons annually.
Additionally less material has to be produced and transported to the forges which would also decrease the CO2-emission.
An economical solution to the conventional forging technologies is the flash reduced forging. It offers several advantages that notably contribute to economic and environmental issues.

[6] This is an average energy consumption, there are no data about the specific energy consumption used by the Euroforge members

These are[4.2]:

- reduced material consumption;
- reduced energy input (reduced material has to be produced and heated up);
- closer tolerances, improving the material utilization and decreasing the allowances for subsequent machining operations.

The best possible flash reduction can be achieved through:

- the development of the pre-forming operations due to the complexity of the part geometries;
- the development of an adjusted temperature distribution of the work pieces e. g. by using a reheating operation;
- the limitations of producible work piece geometries by flash reduced forging process towards the mass deviation along the longitudinal axis.

4.3 The project REForCh[(4.2)]

The aim of the project REForCh is the development of a new resource efficient process chain for high duty parts based on flash reduced forging. It includes pre-forming in closed dies, a multidirectional working die and a conventional finish forging operation. In this way a material utilization of about 90 % can be achieved by having good forging properties and enabling suitable die life-time. Furthermore the needed energy for the process and CO2-emissions will be reduced by save on material and using highly efficient induction heating systems.

The main goal of the heater development is to provide a homogenous temperature distribution in the work piece before pre-forming in closed dies and before the multidirectional forging operation. This is necessary to generate homogenous material properties (these depend on the initial temperature) in the crankshaft after controlled cooling and to reduce the forming force in order to allow a safe machine operation.

The whole process chain including three presses with five dies, an induction heating system, an induction reheating system and an adjusted automatic spraying system will be installed within the project REForCh.

Overall strategy of the work plan

1. Analysis of the products (crankshafts) and production equipment
2. Development of forging sequence
3. Development of the heating equipment
    a. for the induction primary heating: design of the primary heater and dimensioning of process parameters, temperature distribution inside the billet
    b. for induction reheating: temperature distribution inside the work piece with technical details and simulation results of the re-heater design and heating process parameters
4. Forging tools
5. Design and manufacturing of heating equipment for primary heating and reheating
6. Experimental testing
7. Analysis of the work pieces and evaluation of material properties / economical and environmental evaluation
8. Exploitation and dissemination, preparation of IPR documents
9. Management of the project

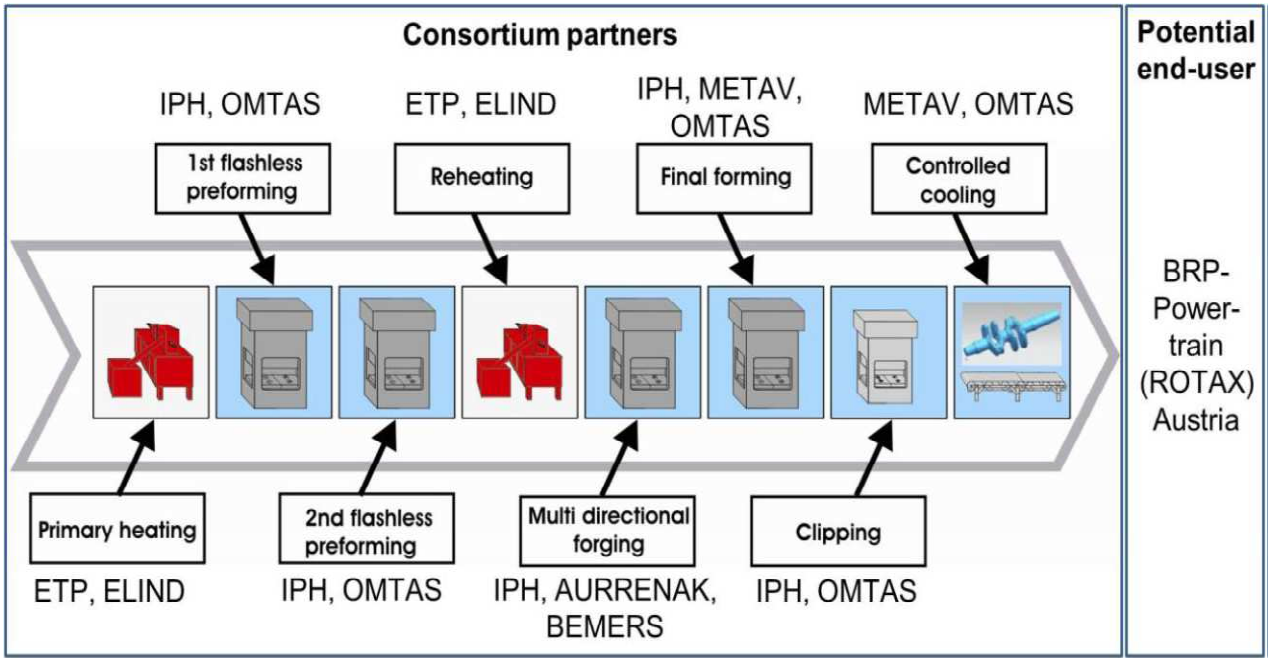

Figure 4.2. *Process chain for flash reduced forging*

4.3.1 Role of the ETP institute

One of the roles of the Institut für Elektroprozesstechnik - Leibniz Universität *Hannover* (ETP) in the REForCh project is the development of the primary heater; this means an optimised concept (heater coil). It will be integrated in the existing heating equipment. The main goal for the primary heater is to be optimized for the optimum raw part geometry and to allow fast heating in order to minimize scale and decarburization on the surface. In flash reduced forging less decarburised material can be pressed out by the flash than at common forging with high flash ratio.

First of all, requirements towards the primary induction heater (steel grade and billet diameter to be heated, required throughput, temperature level and homogeneity) are analysed according to the process specification. A suitable heating concept (linear, non-linear or zone heating) is elaborated and the relevant process parameters are defined regarding the equipment. In particular coil parameters (length, number of sections, diameter, number of windings, coil cross-section, position and number of coil tappings) and the electrical parameters (frequency, power, voltage, and current) are optimised by ETP.

In a second step, a comprehensive numerical simulation model of the primary heating process including analysis of electromagnetic and temperature field as well as the analysis of mechanical stresses (cracks) and scale formation on the surface of the work pieces is developed by ETP.

The aim is determination of the optimal process parameters providing:

- most uniform billet temperature within a short heating time,
- minimum scale formation and surface cracks during the heating and
- reduction of total energy demand, costs and inductor stray magnetic fields.

The second aim is the development of local compensation because of the thermal losses in the work piece caused by the pre-forming operations. The reheating process takes place after pre-forming operations in closed dies (figure 4.2) and provides a billet with an optimised temperature distribution for the multidirectional forging.

A simulation model for the numerical investigation of the electromagnetic and temperature field for the preformed geometry of the work pieces is created by ETP. The model includes an interface for implementation of the non-uniform temperature that occurs after pre-forming operations. Temperature data used for the definition of temperature distributions in the work piece at the beginning of the reheating process are based on measurements performed during the preliminary forging tests and on the results of the forging simulation. The heating concept is defined taking into account the following arrangements of the inductor and work piece:

- fixed work piece with enclosed static inductor;
- fixed work piece with moving inductor;
- fixed inductor with rotating work piece.

Chapter 5

Numerical analysis

Before studying industrial processes, it is important to build a correct virtual model of a machine presents in the laboratory. If the final simulations are describing correctly what is happening in reality, than the model can be adapted to more elaborate situations.

5.1 Presentation of the studied system

During the programming it is not important to understand the losses previous the inductions system (because they are less than 10%), so the only losses are:

- Joule losses in the inductor
- Radiation losses

There are also thermal losses due to the cooling of the water inside the inductors, but during the simulation they are not considered because they present a small percentage and because they don't affect the temperature of the billet.

5.1.1 The coils and the billet

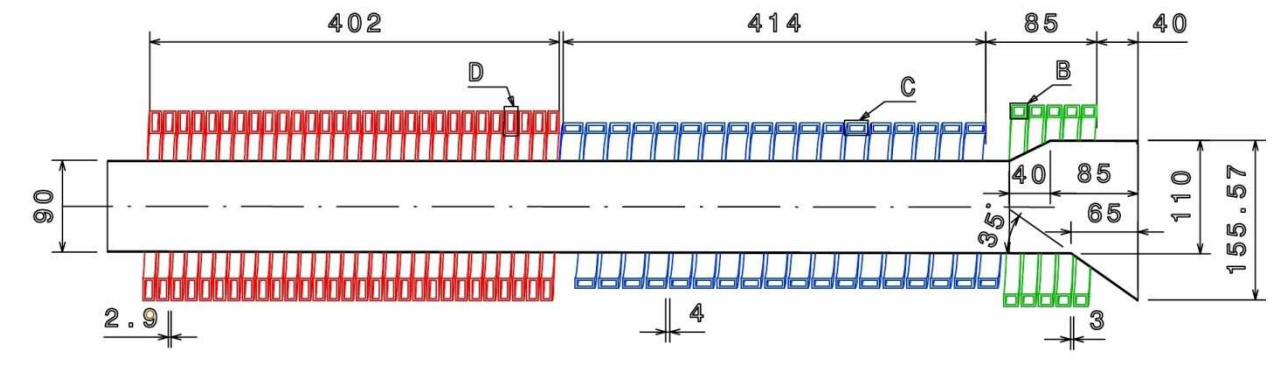

Figure 5.1. *Geometry of the induction coils*

This is a representation of the coils in series inside the generator that will be used during the real experiment. In the simulation and during the experiment the billet is static in the middle of one of the two types of coils (D or C shape). The B detail is not considered.

During the heating, the induction coils are cooled with water rather than oil because the speed of cooling per second is higher with water (also because is simple in case of maintenance). Inside the opening there is a rail cooled with water, on which the billet is placed. Even if not perfectly centred this rails is very important to maintain α as similar as possible to the theoretical value. This water cooled rail has no thermal implications on the billet during the heating.

It is essential to have a realistic geometry of the billet, the refractory and the coils. Especially the last one because, for example, the number of coil can affect the intensity of the magnetic field:

$$H = \frac{NI}{l} \quad (5.01)$$

H - is the intensity of the magnetic field [A/m]
N - is the number of coils in the inductor
I - is the current inside the inductor [A]
l - is the length of the inductor [m]

The generator used for the heating is a BBC Brown Boveri with an input from the line 250kVA, 380V (50Hz), a converter of 200kW at 2000Hz and 500V. The water cooling system has a flow of 5m^2/h and 17600kcal/h. Because of the converter, the frequency applied during the experiment would be lower than 2000Hz.

Figure 5.2. *Generator used for the experiment BBC Brown Boveri*

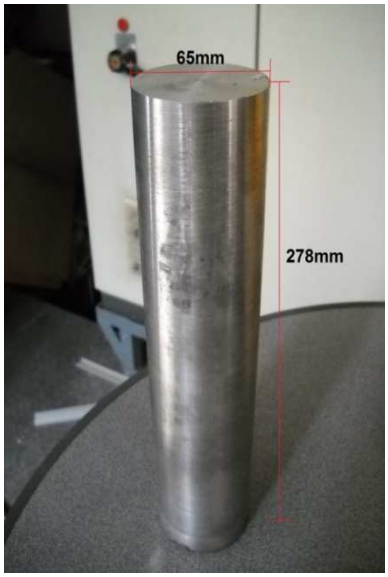

Figure 5.3. *Steel billet*

The billet used during the analysis has the same dimensions (Ø=65mm, L=273mm) and proprieties used during forge processes for the creation of crankshaft for a motor engine (similar process in figure[3.2]). Because of the magnetic nature of the steel, the thermal and electrical proprieties are not linear during the whole heating. The tendency of magnetic materials is to gradually start to change their proprieties when they are reaching a certain value of temperature (Curie point). It is to expect that for steel will be a change in the electrical and thermal proprieties, around 760°C, so the heating will behave differently (Chapter 1 – Induction Theory).

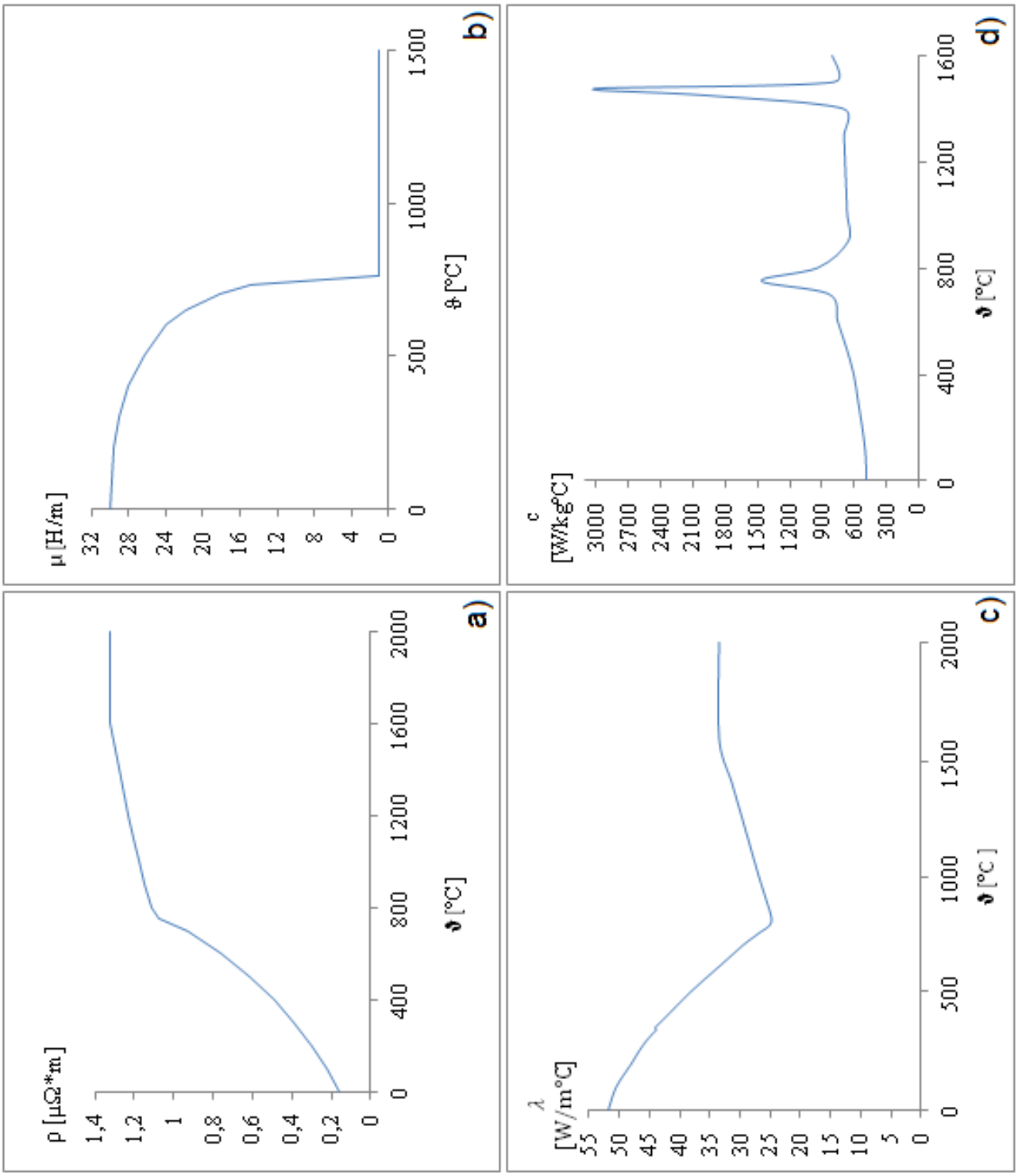

Figure 5.4. *Material proprieties: a) relative resistivity; b) relative permeability; c) thermal conductivity; d)specific heat*

5.1.2 Numerical model

The simulation is made using Ansys 13.0 programming system on a half section 2D model of the billet-refractory-coils system.

The structure of the program must consider the nature of the induction heating process, that means that the analysis is a sequential field coupled analysis of an electromagnetic and a transient thermal analysis. An electromagnetic analysis calculates the Joule heat generation data, and a transient thermal analysis uses to predict the time-dependent temperature solution. The sequential coupled means that results of one analysis become loads for the second analysis, and results of the second analysis will change some input to the first analysis.

Some programming lines of the flow diagram can be seen in the Appendix B2.

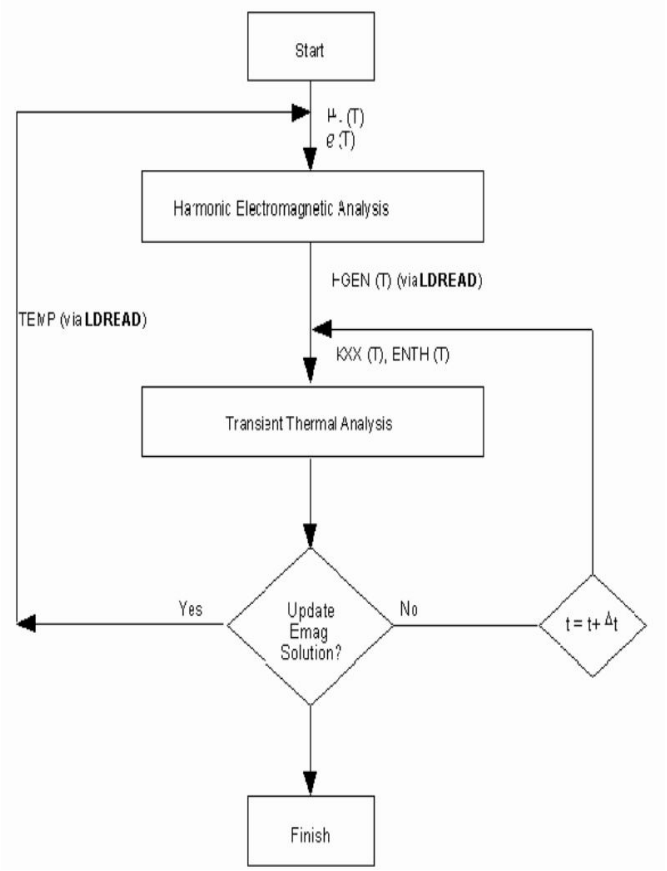

Figure 5.5. *Solution flow diagram*

All the simulations consider one shape of inductor coils during the analysis. But because the real generator has two type of coils (also a third but not with big influence), one is heating the billet (active) and the other one (passive) is still producing a magnetic field. The passive coils are not interfering and there will be no contribution on the magnetic field of the active coils, if it is than is a small contribution that can be not considered during the preparation of the virtual model and in the final results.

The electrical and thermal proprieties of the billet-refractory-coils system are described as function of temperature in the respective files: `prop_elmag.dat` and `prop_therm.dat` (see Appendix B1).

After building the correct geometry of the billet-refractory-coils system, the input file of the program is very simple and can be very easily adapted to answer the changes in the real experiment.

Here is one example of the data input file (`input_transient.dat`):

```
Total_number_of_steps
      53.
 StepNr.     Timestep,s     Runtime,s     I,A
      1.       2.00000       2.00000    1260.00000
      2.       2.00000       4.00000    1260.00000
      3.       2.00000       6.00000    1260.00000
      4.       2.00000       8.00000    1260.00000
      5.       2.00000      10.00000    1260.00000
      6.       2.00000      12.00000    1260.00000
      7.       2.00000      14.00000    1260.00000
      8.       2.00000      16.00000    1260.00000
      9.       2.00000      18.00000    1260.00000
     10.       2.00000      20.00000    1260.00000
     11.       2.00000      22.00000    1260.00000
     12.       2.00000      24.00000    1260.00000
     13.       2.00000      26.00000    1260.00000
     14.       2.00000      28.00000    1260.00000
     15.       2.00000      30.00000    1260.00000
     16.       2.00000      32.00000    1260.00000
     17.       2.00000      34.00000    1260.00000
     18.       2.00000      36.00000    1260.00000
     19.       2.00000      38.00000    1260.00000
     20.       2.00000      40.00000    1260.00000
     21.       2.00000      42.00000    1260.00000
     22.       2.00000      44.00000    1260.00000
     23.       2.00000      46.00000    1260.00000
     24.       2.00000      48.00000    1260.00000
     25.       2.00000      50.00000    1260.00000
     26.       2.00000      52.00000    1260.00000
     27.       2.00000      54.00000    1260.00000
     28.       2.00000      56.00000    1260.00000
     29.       2.00000      58.00000    1260.00000
     30.       2.00000      60.00000    1260.00000
     31.       2.00000      62.00000    1260.00000
     32.       2.00000      64.00000    1260.00000
     33.       2.00000      66.00000    1260.00000
     34.       2.00000      68.00000    1260.00000
     35.       2.00000      70.00000    1260.00000
     36.       2.00000      72.00000    1260.00000
     37.       2.00000      74.00000    1260.00000
     38.       2.00000      76.00000    1260.00000
     39.       2.00000      78.00000    1260.00000
     40.       2.00000      80.00000    1260.00000
     41.       2.00000      82.00000    1260.00000
     42.       2.00000      84.00000    1260.00000
     43.       2.00000      86.00000    1260.00000
     44.       2.00000      88.00000    1260.00000
     45.       2.00000      90.00000    1260.00000
     46.       2.00000      92.00000    1260.00000
     47.       2.00000      94.00000    1260.00000
     48.       2.00000      96.00000    1260.00000
     49.       2.00000      98.00000    1260.00000
     50.       2.00000     100.00000    1260.00000
     51.       2.00000     102.00000    1260.00000
     52.       2.00000     104.00000    1260.00000
     53.       2.00000     106.00000    1260.00000
```

The area with air proprieties has a conventional fixed value of temperature (20°C) to represent the thermal losses of the billet with the environment. While the initial temperature of the billet is set to 0°C because the initial propriety values start from that temperature. This does not affect the simulation, because anyway with the current used after 2 seconds the temperature is around 100°C even if the initial temperature of the billet is 20°C.
The frequency value is fixed and directly written inside the file dedicated to the geometry.
If the electrical input chosen is the voltage than some program lines should be written to calculate the current inside the inductors, but this can increase the time machine for the elaboration of the simulation's data. In case of the current the simulation is faster.
The current (or voltage depending on the type of chosen input) are the only data that can be modify in each time step.
It is very important to select a good numbers of time steps because it defines how accurate the simulation can be. There are few things to consider:

- it is important not to have less than 30 steps because the time for every step is to big and some information can be lost and bring to wrong results;
- too many steps increase significantly the time of elaboration of the data;
- time steps around the Curie point should be small because it is a crucial moment during the heating.

The program produces different kind of output files:

- isotherms imagines of the load for every time step;
- `control.dat` file with the temperatures for each time step of the selected points of study;
- `out_temp_cross.dat` file with the cross section temperature data;
- `electric_data.dat` file with electrical information (current applied, power load-inductor, power load, electrical efficiency and power factor) for each time step.

5.1.3 Data recovery

During the experiment two thermocouples[7] are used, both of them are along the middle of the length: one on the axis and the other on the surface. To prevent damaging the thermocouples, the heating must be turn of before the temperature reaches 1100°C.
The temperatures, voltages and frequencies values collected from the thermocouples are taken every 1,2 seconds and stored in the computer for later comparison with the values obtained from the simulation.
In table[5.1] the time is approximated to a significant value and the voltage is already converted because the output from the thermocouples is expressed in mVAC.

[7] Base on the Seebeck effect, a thermocouple can register the electrical potential produced during the heating of two conductors. A thermocouple is made of two electrical conductors of different materials put together in one point (*hot junction*) on the other side the two materials are separated (*cold junction*). If the temperature is different in the two junctions, it is possible to analyse the voltage on the *cold junction* that is directly proportional to the temperature thorough this equation: $\Delta T = \sum_{n=0}^{n} a_n V^n$ where a_n depends on the materials used

Tabel 5.1. *Data acquired during the experiment*

Time(s)	Voltage(V)	Frequency(Hz)	Out Temperature (°C)	Inside Temperature(°C)
0	187	1786,1297	114,711	29,503
2	207	1817,7184	133,911	37,656
3	221	1823,296	151,123	31,696
5	239	1840,6461	192,59	35,007
7	257	1876,2066	233,052	38,137
9	271	1866,913	269,775	63,894
10	281	1883,6893	297,295	72,105
12	285	1886,7105	356,349	51,377
14	285	1887,282	392,808	91,82
15	284	1887,3134	433,283	87,226
17	283	1887,6841	476,26	99,336
19	283	1899,7379	510,603	115,177
21	286	1884,4813	542,617	152,484
22	291	1913,284	569,718	170,357
24	305	1922,7221	606,684	176,42
26	336	1952,849	627,005	218,211
28	376	1978,1276	654,254	237,882
29	422	1998,7599	667,142	271,531
31	448	1995,4002	694,133	289,566
33	432	1957,1455	708,936	323,212
34	402	1949,1752	724,721	366,358
36	375	1933,2815	740,369	374,627
38	349	1918,4665	736,467	415,998
40	325	1899,102	740,27	442,88
41	331	1901,4747	741,039	467,996
43	343	1910,666	736,9	481,364
45	357	1937,2455	738,366	523,382
46	364	1917,7961	753,077	520,175
48	364	1916,0844	743,346	536,477
50	362	1915,4982	746,152	556,654
52	362	1924,8763	756,759	589,781
53	360	1913,2173	752,814	582,684
55	360	1921,3886	762,919	613,598
57	358	1930,4343	759,819	606,108
59	356	1909,0734	765,464	632,755
60	356	1908,3049	761,702	632,554
62	356	1917,3537	768,444	655,386
64	355	1906,6091	767,178	656,65
65	355	1905,9083	766,642	661,828
67	355	1915,2371	766,736	680,303
69	355	1914,7564	770,097	678,812
71	355	1904,0843	773,49	695,83
72	355	1913,6241	775,078	694,584
74	355	1913,2904	777,928	705,889
76	355	1912,7154	778,606	713,537
77	354	1902,4122	783,509	720,088
79	354	1902,2543	785,602	722,882

81	354	1911,9249	789,118	726,367
83	354	1901,541	791,594	734,684
84	354	1901,44	796,828	737,254
86	354	1911,4206	801,114	742,412
88	354	1901,399	805,043	746,725
90	354	1901,5346	808,564	749,947
91	354	1901,8628	812,879	754,892
93	354	1901,9607	817,324	761,075
95	354	1902,0649	822,964	766,733
96	354	1902,3427	826,576	769,061
98	354	1912,5852	831,6	774,358
100	354	1912,7027	837,395	782,473
102	354	1912,5788	843,974	789,948
103	354	1922,553	848,551	790,655
105	354	1912,5598	855,194	802,649
107	354	1912,6614	859,593	810,13
109	354	1912,6042	865,096	820,244
111	354	1912,4772	871,046	831,943
112	354	1912,4772	877,102	839,27
114	354	1922,4763	881,527	844,484
115	354	1912,6074	889,099	852,895
117	354	1912,7916	892,289	867,713
119	354	1902,7818	898,563	876,14
121	354	1903,0946	902,133	881,493
122	354	1923,1341	908,949	888,122
124	354	1903,4233	913,6	899,764
126	355	1913,3476	920,787	909,428
127	355	1913,4397	926,374	911,486
129	355	1903,3917	933,304	915,127
131	355	1913,427	934,326	927,357
133	355	1913,4556	943,887	932,856
134	355	1923,4982	946,349	939,74
136	355	1913,64	952,68	952,129
138	355	1913,6527	955,436	953,951
140	355	1913,8466	963,148	965,7
141	355	1904,2393	968,43	974,758
143	355	1914,2537	970,936	980,068
145	355	1914,2728	979,945	980,866
146	355	1914,0088	981,28	988,961
148	355	1914,4636	986,396	1001,169
150	355	1914,33	995,748	1007,402

5.2 First experiment

The billet is set in the middle of the D shape inductor (22x11x2mm), with a section of 402mm long and has 29 coils. Theoretical α is 2,15. In the real geometry the billet is not perfectly centered because of the cooling rail on which the billet stays, but this does not change the α parameter.

During the heating the average current will be 1000A while the frequency starts with a low value and increases until 1914Hz because of the start up time of the generator.

After retrieving the data from the experiment a simulation was made with the same conditions.

The diagram shows how, during the experiment, is changing the temperature on the surface (*out temp*) and along the axis (*in temp*) of the billet.

In the beginning of the heating the skin effect (δ) is 2,06mm, this means that the temperature on the surface is higher than the core because of the higher density of the current (1.1 Electromagnetic Theory). After the Curie point (figure[5.4]) the proprieties of the material change and so it is expected to have a slow rise of the temperature.

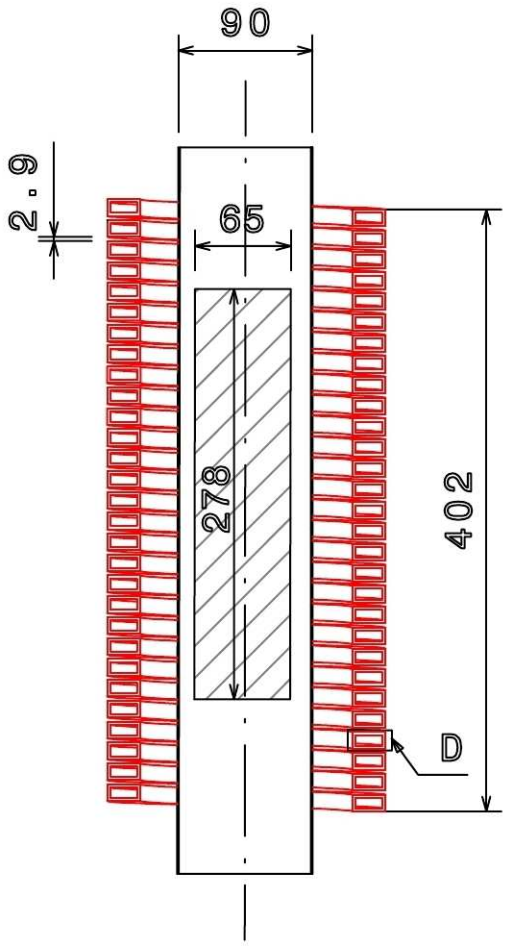

Figure 5.6. *First experiment geometry*

The comparison (figure[5.7]) of the surface temperature values obtained from the real analysis and the simulation (*out simul*) show that ΔT between the temperatures (*out diff*) is a little higher than 50°K, but after few seconds it stars to fall down and at the end of the heating the final temperature is almost similar.

Around the Curie point, the temperature gap between simulation and real data is higher because of two things:

- not complete accuracy of the proprieties for the simulation, it is very difficult to predict the correct values in this transient;
- at the beginning of the experiment (first twenty seconds), because of the start up system of the generator, the frequency starts with a low level and then it stabilizes.

The main contribution for this gap difference comes from the first point, while the second is less effective.

At the same time the temperature along the axis is raising but the values are lower at the same moment, because with $m > 20$ current density is low.
A comparison of the real (*in temp*) and the simulated (*in simul*) temperature shows how the values are inside the ±50°K range until around 105 seconds. After this time the *in temp* is raising too fast and the *diff in* value is above ±50°K.
To better adapt the simulation and lower down this difference, the proprieties of the refractory were changed. But even applying these changes the results are the same.
This increase is unexpected also for a theoretical point of view. If the process is enough long the temperature on the surface can be lower than the core because the thermal losses on the surface become higher than the heating. This is not the case because the time is still short.

Figure 5.7. *Data retrieved from the experiment and the simulation of a steel billet heated with D shape coils*

Because of the magnetic nature of the billet, the global electrical efficiency is a composition of the efficiencies before (η_A) and after (η_B) the Curie point.

$$\eta_e = \frac{\eta_A t_A + \eta_B t_B}{t_A + t_B}$$

With this inductor η_e = 71,6%

The figure[5.8] shows how the global efficiency is changing during the heating: in a first moment (~35s) the value is rising to 85% and after it starts to fall because on the surface already reached the Curie point while the electrical proprieties are still changing inside the material.

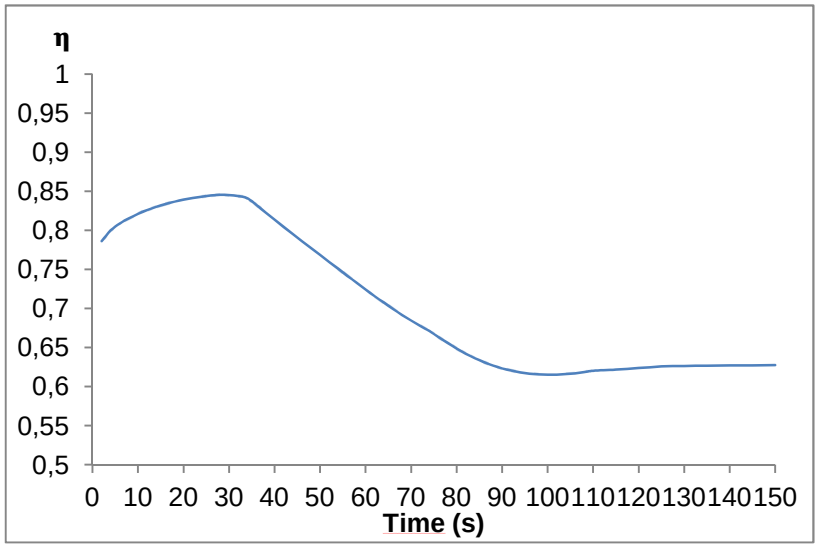

Figure 5.8. *Variations in the simulation's global electrical efficiency*

After 90 seconds also the core is reaching the Curie temperature and gradually is changing proprieties, than stabilizing around 64%.

It is also possible to check the trend of the power factor during the entire heating.

$$cos\phi = \frac{r_i + r_c'}{\sqrt{(r_i + r_c')^2 + (x_{i0} + \Delta x)^2}} = \frac{1}{\sqrt{1 + \left[\frac{\alpha^2 - (1 - \mu B)}{\mu A}\eta_e\right]^2}}$$

During the process the power factor is very low, because of α. This is compatible with the values seen in the theory (figure[1.6]). The power factor must be considered to avoid problems on the supply line, because usually the power factor has to be around 0,8÷0,9. In this case the right number of capacitors must be put.

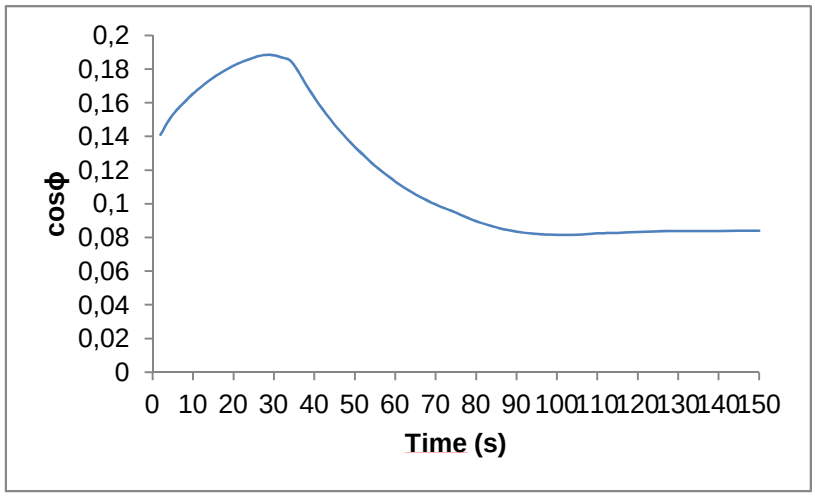

Figure 5.9. *Power factor of the load-inductor*

5.3 Second experiment

The billet is set in the middle of the C shape inductor (10x19x2mm), with a section of 414mm long with 18 coils.
During the heating the average value of frequency is ~1870Hz. For this experiment the average current value is around 1275A. But because of the lower number of coils and a slightly higher current used, the time of the heating will be longer due to the lower magnetic field produced. The time expected to reach a temperature of 1000°C is around 300 seconds.
The working limitations are the same as seen in the previous experiment.
After retrieving the data a simulation is made with the same conditions to compare the results.

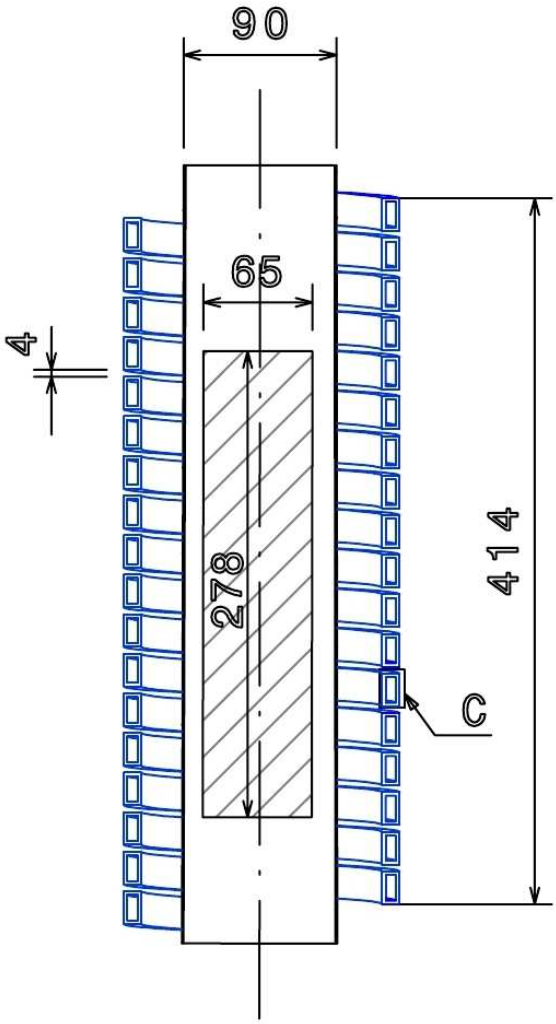

Figura 5.10. *Second experiment geometry*

Unfortunately during the process the thermocouple on the surface was damaged and the comparison of the data in the final moments of heating are meaningless.
For the same reasons seen in the first experiment, before the Curie point the temperature difference (*diff*) is above the ±50°K.
After this critical point the two temperatures have a similar trend and the difference is becoming very small at the end of the heating. In this final moments it is not found a big temperature difference as in the previous experiment.

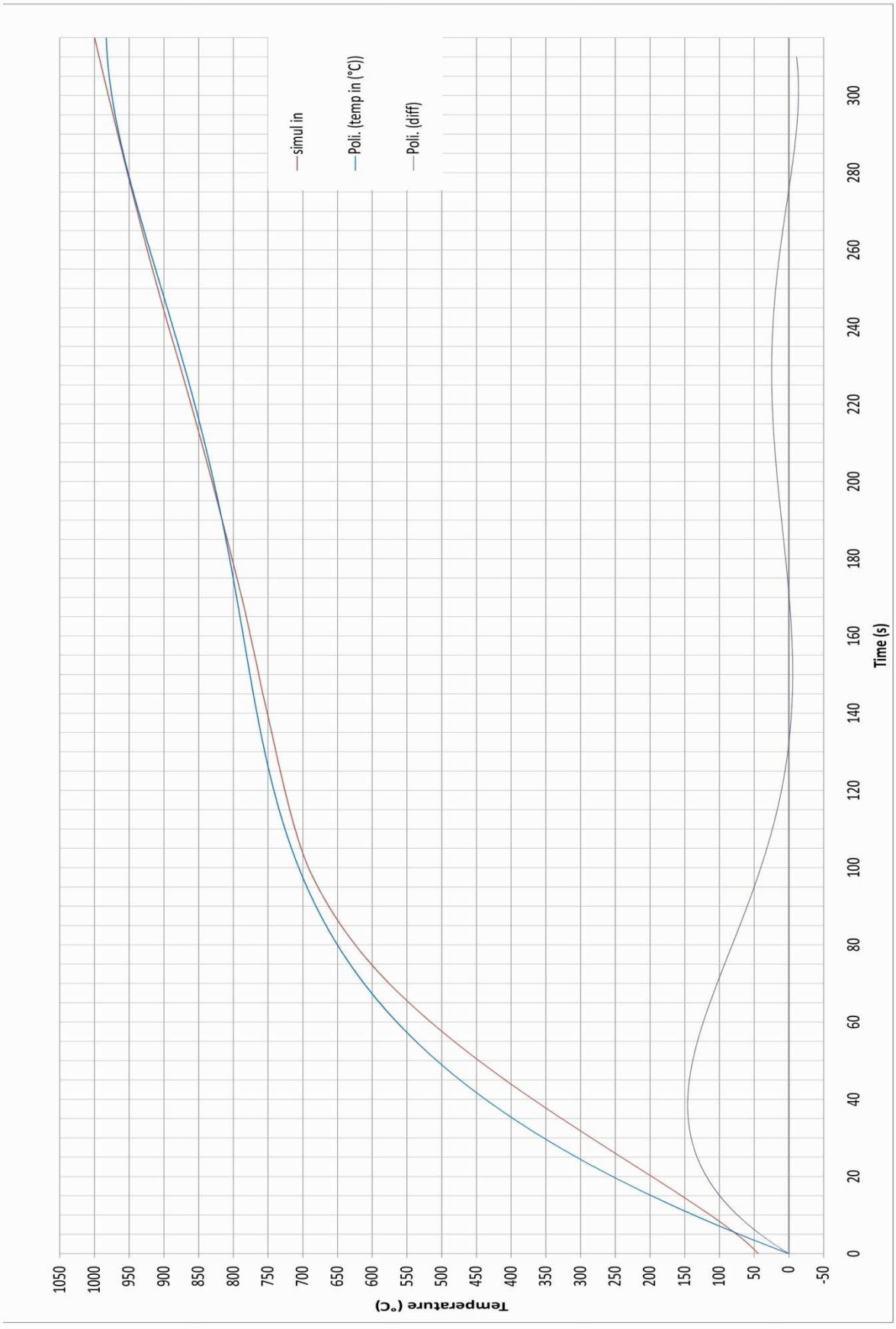

Figure 5.11. *Data retrieved from the experiment and the simulation of a steel billet heated with C shape coils*

Global efficiency is acting as expected and the results are similar to the first experiment.
With this inductor the global efficiency is higher η_e = 75,2% compared to the previous case.

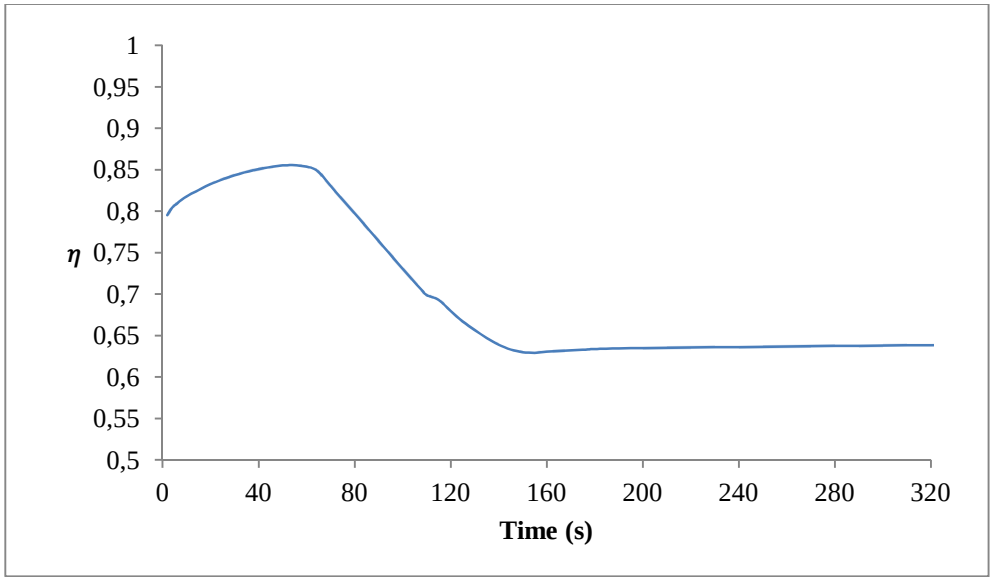

Figure 5.12. *Variations in the simulation's global electrical efficiency*

In this case because of the lower magnetic field applied the time needed is longer but the behaviour is the same as seen previously.
Also the power factor has the same behaviour and the same values as seen in the first experiment.

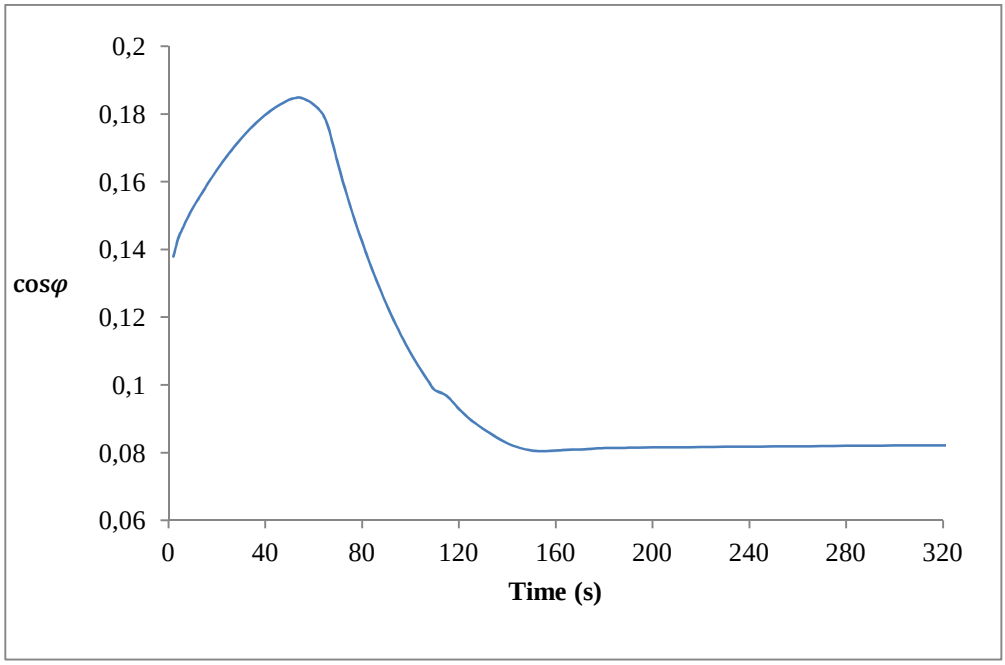

Figure 5.13. *Power factor of the load-inductor*

Chapter 6

Application of the model

With the validation of the virtual model, it is possible to create some simulations introducing some of the goals that are used in the heating process of the REForCh project.
The goals are:

- Temperature not higher than 1200°C (to avoid melting problems)
- Time for the process not higher than 300s
- Difference between surface and core $\Delta T=20\div30°K$

With this goals in mind, it is now possible to do some simulations on the generator used (BBC Brown Boveri) and obtain the best values for the heating of the steel billet (Ø=65mm, L=273mm) in a very simple industrial process. Because of the generator used, the frequency applied in the simulation is 2000Hz.
The fixed value of frequency and geometry leaves only the possibility to change the current applied in the inductors.

6.1 Simulations

6.1.1 D coils

The first few simulations are made with the D shape inductor, with an input of currents that have a range from 900A to 1000A and put together in figure[6.1].

Tabel 6.1. *Temperature values in the final moments (before 300s) obtained with different input of current*

Time(s)	900A Outside and inside temperature (°C)		925A Outside and inside temperature (°C)		950A Outside and inside temperature (°C)		1000A Outside and inside temperature (°C)	
230	1053	1014	1083	1043	1117	1077	1180	1138
240	1071	1035	1102	1065	1137	1100	1202	1163
250	1089	1056	1122	1087	1157	1123	1224	1188
260	1107	1076	1140	1109	1177	1145	1245	1213
270	1125	1096	1159	1130	1196	1167	1266	1236
280	1142	1116	1177	1150	1214	1188	1287	1259
290	1159	1135	1194	1170	1233	1208	1307	1282
300	1175	1153	1211	1189	1251	1229	1327	1304

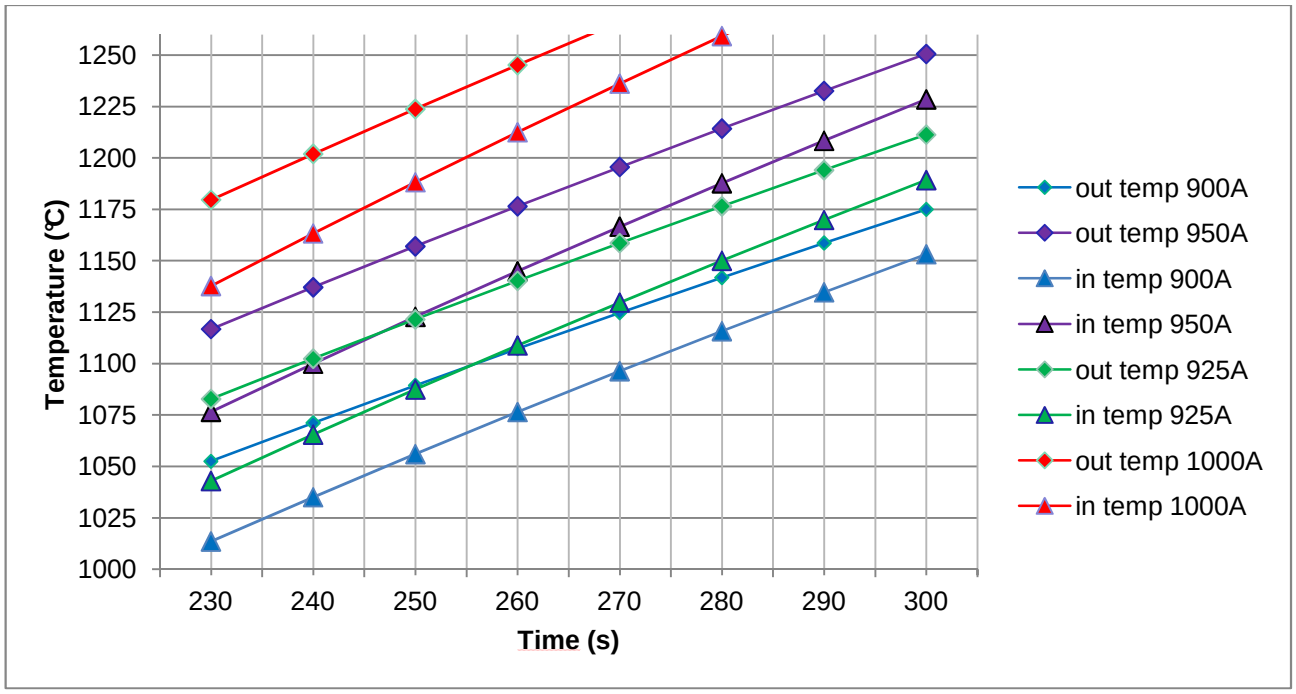

Figure 6.1. *Temperature evolution in the final moments of heating using different currents*

On a first look seems that all the simulations (except the one with 900A) are good because the final temperature on the surface reaches 1200°C before 300 seconds. But also temperature differences must be checked to fulfil the last requirement. In figure[6.2] can be seen the time when the ΔT has a value that is lower than 30°K.

It is possible to discard the simulation with 1000A because ΔT<30°K after 270s but the temperature on the surface is above 1200°C, that is in conflict with one of our goals.

The simulations with 925A and 950A have ΔT<30°K after 266s and the *out temp* <1200°C, between both the best one is with 950A because in the same time the temperature in the billet is higher than in the other one and so the heating process for the billet is faster.

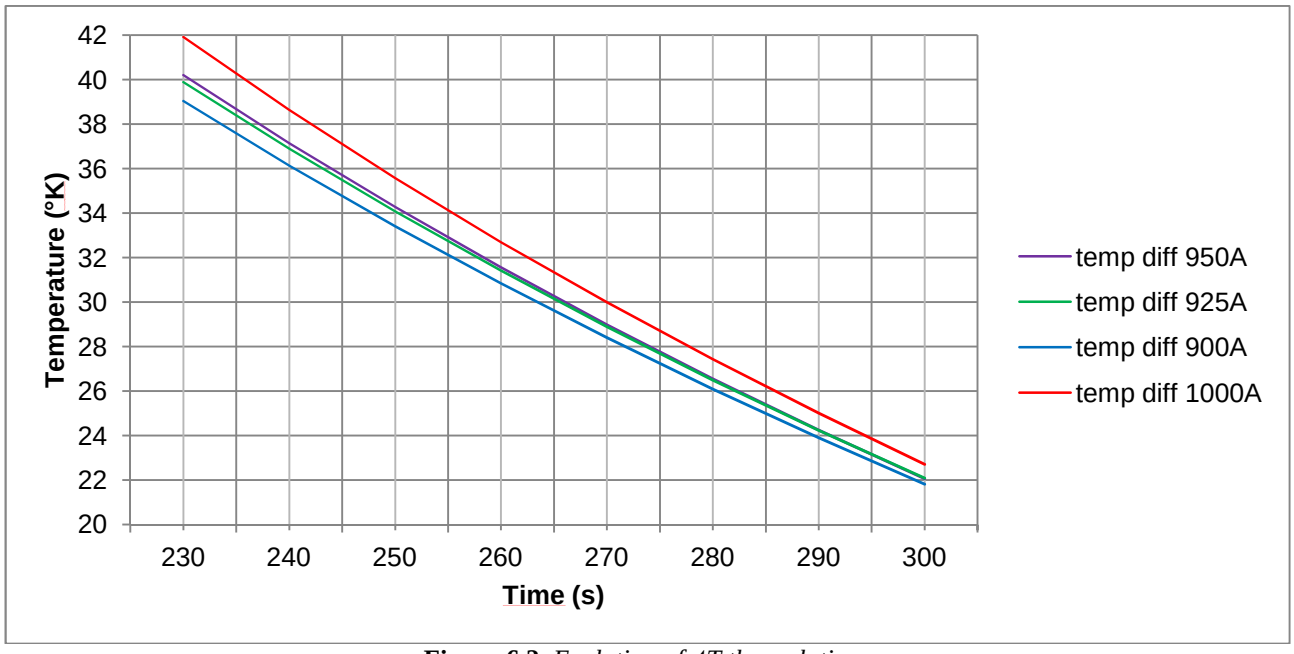

Figure 6.2. *Evolution of ΔT through time*

A view of the cross section figure [6.3] of the billet after 265s shows how the distribution of the temperature is.
The skin effect is δ=0,01247m, this means that the majority of the current is between ~0,02m and the surface.

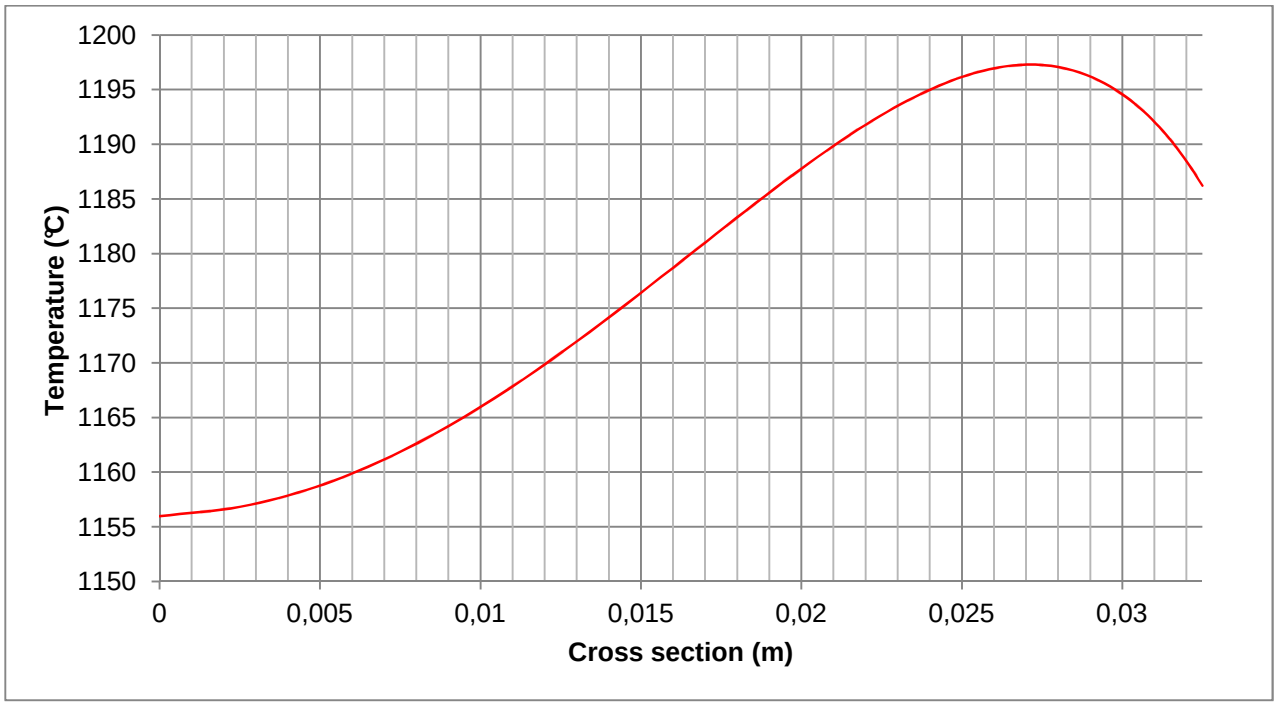

Figure 6.3. *Cross section of the billet after 265s with an input of 950A*

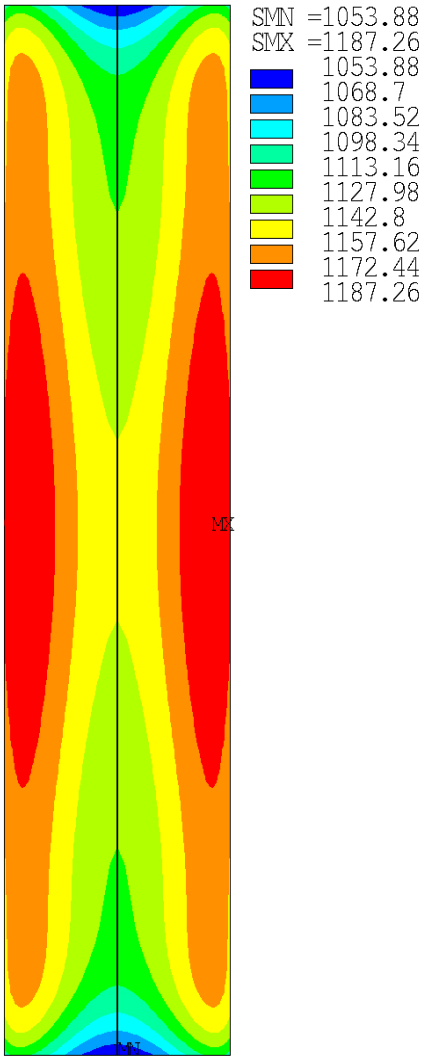

Figure 6.4. *Temperature cross section*

Another thing that should be considered, are the thermal losses between the billet and the air, because the temperature on the surface is little lower than few millimetres inside the billet. If this is not considered than some parts inside the billet can melt and create defects in the final product.

The cross section in figure[6.4] of a billet after 265 seconds show how is distributed the temperature inside during the final moments of heating.

The difference between the coolest (blue colour) and the hottest (red colour) point inside the billet is more than 120°K. The reason why the blue spots are in the middle of the circular surface of the billet is the contribution of two factors: one is the distribution of current density along the axis (r=0 or ξ=0) that is lower compared to the surface (low heat generation inside the billet), while the other is the thermal losses to which it is subjected. This combination of factors creates a big temperature inequality.

This is acceptable because it is taken in account with the $\Delta T=20\div30°K$ between surface and core, and also the interested volumes are very small compared to the rest of the billet.

6.1.2 C coils

For the simulations concerning the C detail inductor was taken a range of currents that goes from 1500A to 1600A, because the field is lower than in the previous type of inductor, and put together in figure[6.4] that shows the temperatures trend in the final moments (before exceeding 1200°C).

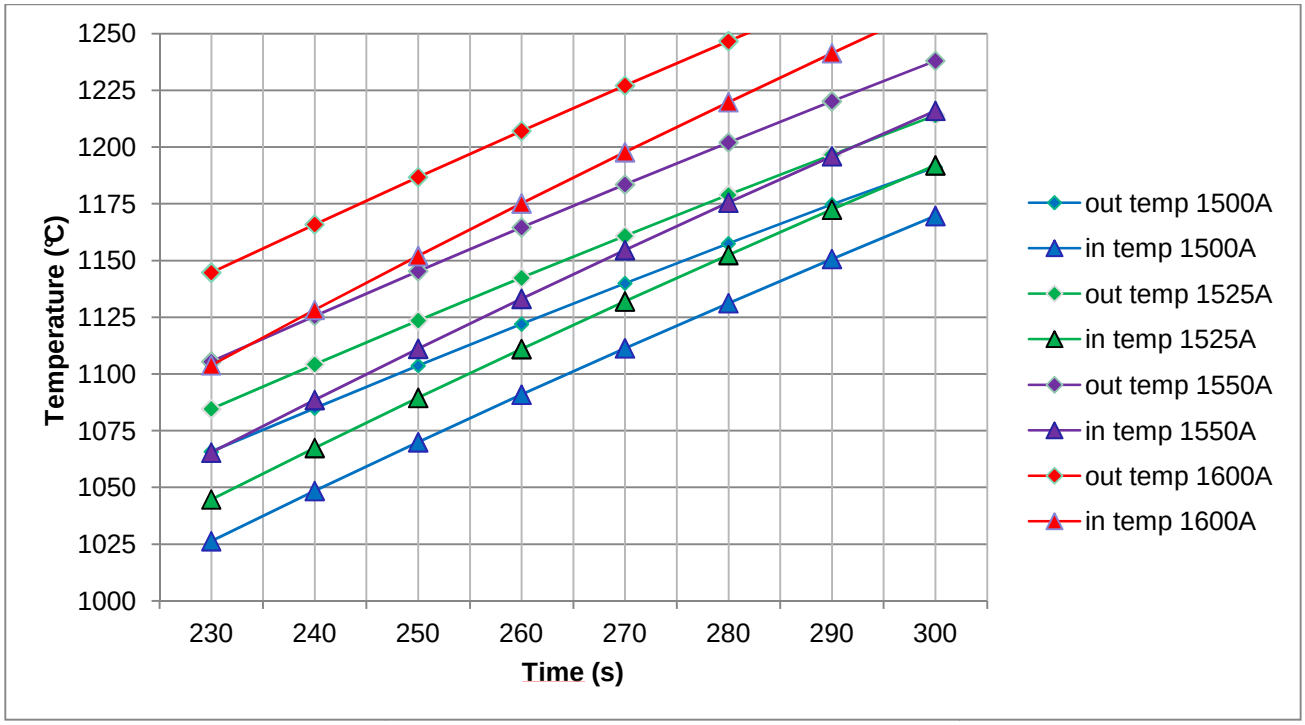

Figure 6.4. *Temperature evolution in the final moments of heating using different currents*

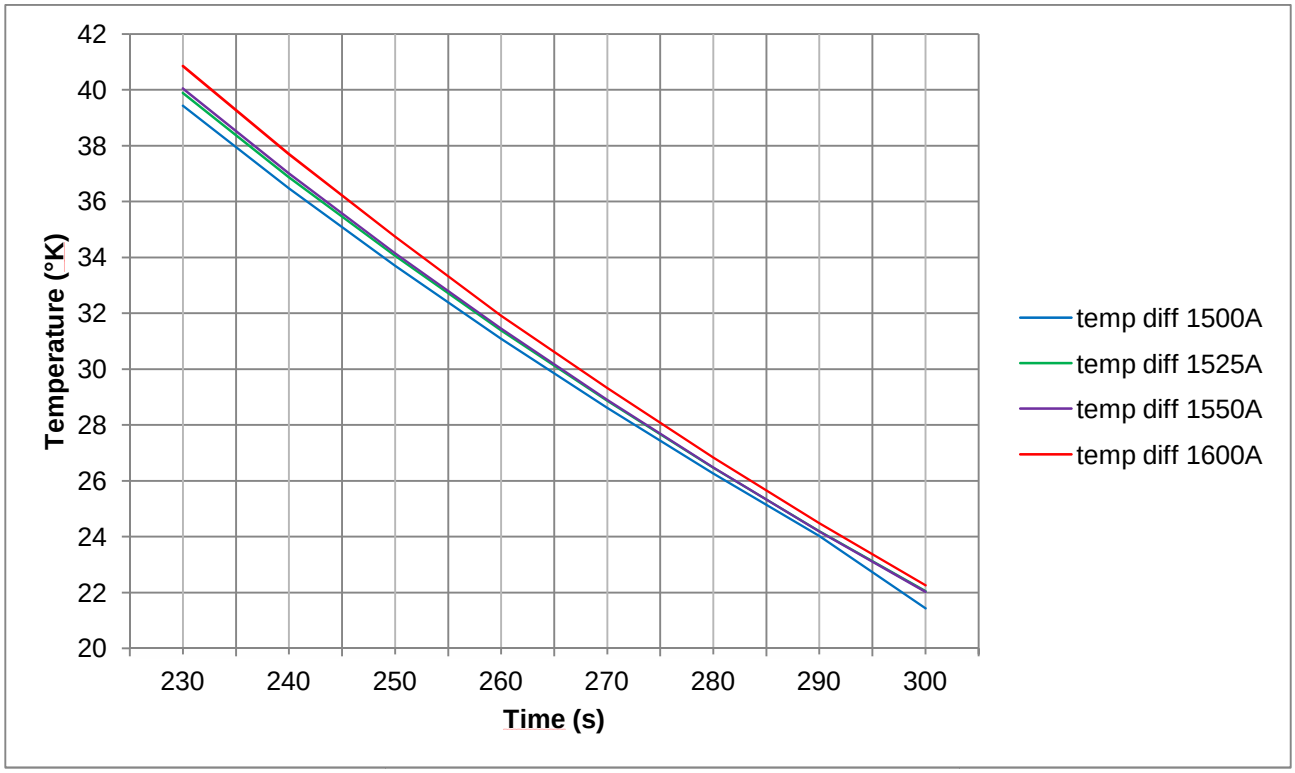

Figure 6.5. *Evolution of ΔT through time*

The same considerations must also be made to choose the right values for this kind of inductor. The simulations with 1600A shows that $\Delta T<30°K$ after 267s, when the temperature is already above 1200°C.
The best values is with 1550A because $\Delta T<30°K$ is around 265s and the temperature is lower than 1200°C.
With 1500A and 1525A the heating needs a few more seconds and the difference in power needed is less than few KW.
View of the cross section of the billet heated with 1550A.

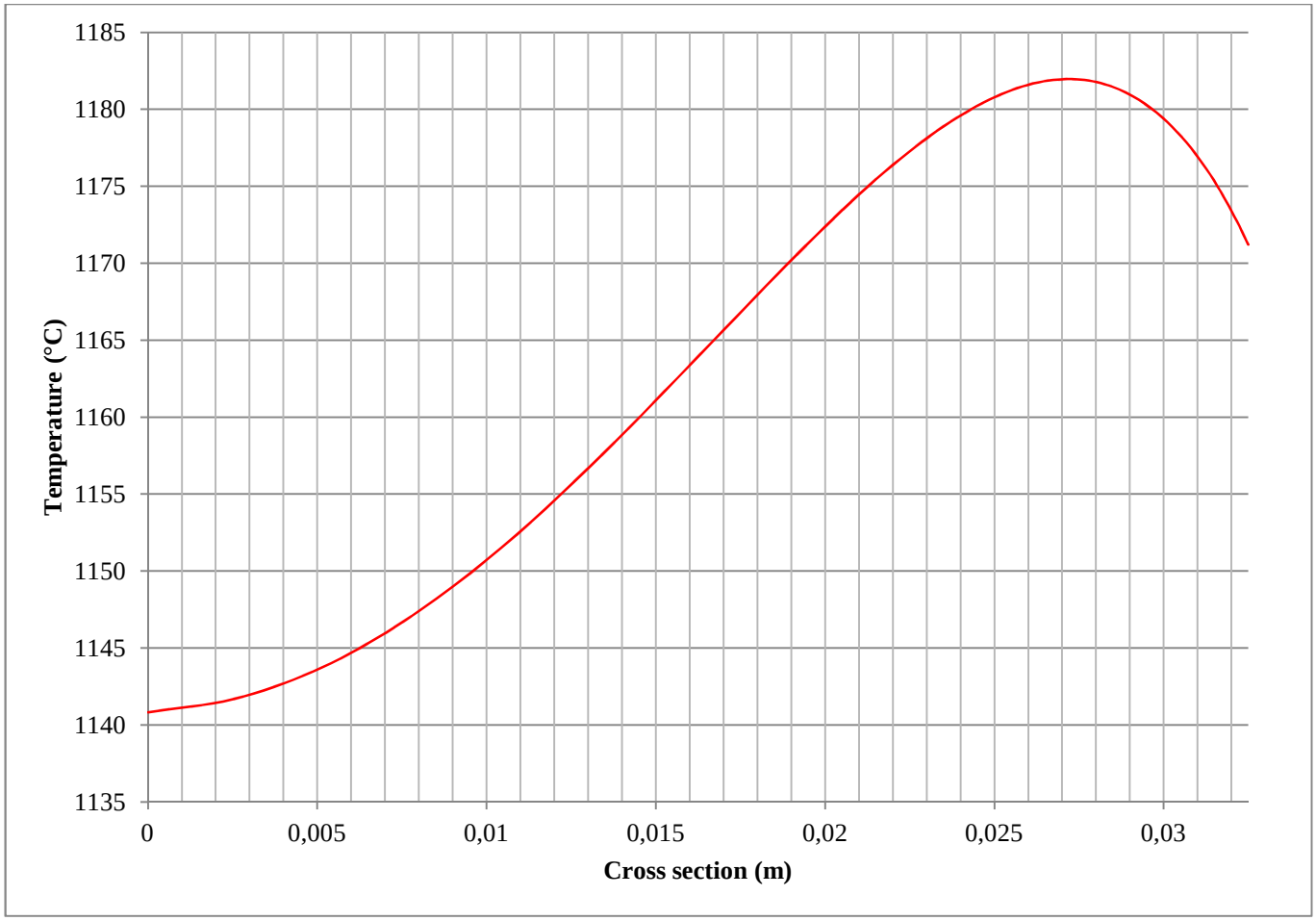

Figure 6.6. *Cross section of the billet after 265s with an input of 1550A*

6.1.3 Considerations

A small comparison of the electrical results (Appendix C) between the D coils (950A) and C coils (1550A) shows that in the first case the average efficiency is 67,7% and the power factor is 0,1 while for the second case the results are an efficiency of 68,7% and a power factor of 0,098.
Also the average power needed for heating the billet is very close in both cases.
To reach the same temperature and times, the choice for the right inductor can be based on economical factors like: the cost for the copper used for the inductors, the cost for the generator, the number of capacitors to raise the power factor and energy saved.

Chapter 7

Final considerations

Theoretical studies and practical experiments demonstrate that the numerical modelling of industrial heating e.g. of steel billets is a reliable tool for the design of induction heating equipments. Numerical models are based on the flow diagram presented in figure[5.5] where all the most important characteristics of the workpiece during the heating are taken into account, mostly the temperature dependence of material proprieties.

Results of numerical models have been compared with data collected from experiment with D coils and C coils, with a tolerance that should not exceed ±50°K especially at the end of the heating.

If real temperatures are different this could create problems during subsequent processing because the material does not have the required proprieties.

The comparison of data of the D coils inductor (figure[5.7]), shows a sudden increase of *in temp* that goes above the tolerated limits. Some verification were made after this results with the program, precisely modifying the material proprieties of the refractory, but there were no significant changes.

A first conclusion is that the thermocouple, used to measure the temperature along the axis, registered an anomaly due to the short time of the process or simply it had a malfunction.

This is confirmed after the comparison of the data of the C coils inductor (figure[5.11]). In this case the sudden increase of *in temp*, is not present. In fact with a longer heating the temperatures are inside the tolerance limits.

In both of the experiments there is discrepancy in the trend before the Curie point due to the numerical model limitations.

The first one is the difficulty of obtaining accurate data for material proprieties while the temperature is changing, this means that some of them must be interpolated by the program creating a small error.

The second limitation is the fixed frequency value used by the numerical model that must be selected as an average frequency during heating because the generator needs time, this means that the initial frequency is different (lower) than the value at the end of the heating.

A third one can be the difference in the starting temperatures during the experiments from the simulations because of the not state of the art conditions.

The contribution of each of this three creates small errors, but it is important that the simulated final temperatures of the surface and axis are inside the tolerance value.

Even if the virtual model describes a quirt simple process, because during the simulation the billet is not moving and it is heated with only one type of inductor, it can be implemented to simulate and

calculate more complicated situations (like real production lines) where the billet is moving along a rail thorough at least two different type of inductors.
For the replication of industrial processes, it is required more time for the creation of the program and adequate machinery for practical testing.

Appendix A

Symbols

	Symbol	Unit
Length	l	m
Current	I	A
Voltage	U	V
Temperature	ϑ	°C
Surface Temperature	ϑ_s	°C
Axis Temperature	ϑ_a	°C
Relative Resistivity of Load	ρ	Ωm
Relative Resistivity of Inductor	ρ_i	Ωm
Number of coils	N	-
Frequency	F	Hz
Magnetic Permeability	μ	H/m
Magnetic Permeability Constant	μ_0	H/m
Intensity of Electric field	E	V/m
Intensity of Magnetic Field	H	A/m
Current Density	G	A/m^2
Thermal Conductivity	λ	W/m°C
Specific Heat	c	W/kg°C
Skin Effect Depth	δ	-
Global Efficiency	η	-
Power Factor	$\cos\varphi$	-
Power	P	W
Power	P_u	W/cm
Energy	E	Wh

Appendix B

Program

Appendix B1 Proprieties

`prop_elmag.dat` the electromagnetic proprieties

```
mptemp
mptemp,1, 0, 200, 300, 400, 500, 600
mptemp,7, 650, 700, 730, 760, 2000, 200000

mpdata,murx,201,1, 30.0, 29.54, 29.13, 28.11, 26.29, 23.94
mpdata,murx,201,7, 21.79, 18.08, 14.75, 1.0, 1.0, 1.0

mptemp
mptemp,1, 0, 100, 200, 300, 400, 500
mptemp,7, 600, 700, 750, 800, 900, 1000
mptemp,13, 1100, 1200, 1400, 1600, 2000, 200000

mpdata,rsvx,201,1, 16.0e-08, 22.1e-08, 29.6e-08, 38.7e-08, 49.3e-08, 61.9e-08
mpdata,rsvx,201,7, 76.6e-08, 93.2e-08, 107.9e-08, 111.1e-08, 114.9e-08, 117.9e-
08
mpdata,rsvx,201,13, 120.7e-08, 123.0e-08, 128.0e-08, 132.0e-08, 132.0e-08,
132.0e-08
```

While for the other material the permeability has a unit value.

`prop_therm.dat` the thermal proprieties of the entire geometry

```
!steel
mptemp
mptemp,1, 0, 100, 200, 300, 400, 500
mptemp,7, 600, 700, 750, 800, 900, 1000
mptemp,13, 1100, 1200, 1400, 1600, 2000, 200000

mpdata,kxx,201,1, 51.9, 50.6, 48.1, 45.6, 41.9, 38.1
mpdata,kxx,201,7, 33.8, 29.5, 27.0, 24.8, 25.7, 26.9
mpdata,kxx,201,13, 28.0, 29.1, 31.3, 33.5, 33.5, 33.5
mptemp
mptemp,1, 0,100, 200, 300, 400, 500
mptemp,7, 600, 700, 750, 800, 900, 1000
mptemp,13, 1100, 1200, 1300, 1400, 1450, 1475
mptemp,19, 1500, 1600, 200000

mpdata,c,201,1, 480, 490, 520, 560, 600, 670
mpdata,c,201,7, 750, 830, 1460, 930, 650, 660
mpdata,c,201,13, 670, 680, 690, 700, 2000, 3000
mpdata,c,201,19, 780, 800, 800

mp,dens,201,7800
```

```
alphaworkpiece=10
emissworkpiece=0.8

!refrectory

mptemp
mptemp,1, 0, 20, 1400, 200000

mpdata,kxx,501,1, 1.2, 1.2, 2.0, 2.0

mp,c,501,400.0
mp,dens,501,2500

alpharef01=10.0
emissref01=0.8
```

Appendix B2 Harmonic electromagnetic analysis and transient thermal analysis

The begin of the electromagnetic part

```
/clear
/FILNAME,BATCH_U,1
resume,environment_emag,db
/input,iiii,dat
/input,current,dat
   /assign,rst,BATCH_U,rmg
   /solu
   csys,0
   allsel,all

    *if,iiii,eq,1,then
      tunif,20
    *else
      ldread,temp,last,,,,,rth
    *endif

      current=input_transient(iiii,5)
      currentm_r=current*1.414213562
      currentm_i=0.0

csys,0

nsel,s,loc,y,y0-eps,y0+eps
d,all,az,0,0
   nsel,s,loc,y,y3-eps,y3+eps
   d,all,az,0,0
      nsel,s,loc,x,x0-eps,x0+eps
      d,all,az,0,0
         nsel,s,loc,x,x3-eps,x3+eps
         d,all,az,0,0

*do,ii,1,w_n01,1
   esel,s,mat,,(1100+ii)
   nsle
   cp,next,volt,all
      esel,s,mat,,(1100+ii)
      nsle
      *GET,nmin,NODE,0,NUM,MIN
```

```
      f,nmin,amps,currentm_r,currentm_i
*enddo

esel,all
nsel,all

   antype,harmic
   harfrq,frequency
esel,all
nsel,all

solve
finish

/POST1

SET,,,1,0,,
vrealsum=0.0
*do,ii,1,w_n01,1
   esel,s,mat,,(1100+ii)
   nsle
*get,nmin,NODE,0,num,min
*get,vreal,NODE,nmin,VOLT
vrealsum=vrealsum+vreal
*enddo

SET,,,1,1,,
vimagsum=0.0
*do,ii,1,w_n01,1
   esel,s,mat,,(1100+ii)
   nsle
*get,nmin,NODE,0,num,min
*get,vimag,NODE,nmin,VOLT
vimagsum=vimagsum+vimag
*enddo

vsum=sqrt(vrealsum*vrealsum+vimagsum*vimagsum)
voltage=vsum*2*3.14159265*frequency/1.414213562

*if,vsum,le,0.0,then
cosphi=0.0
*else
cosphi=abs(vimagsum/vsum)
*endif

finish

/POST1

SET,,,1,0,,

runtime=input_transient(iiii,3)
vy=input_transient(iiii,4)
esel,all
powerh
realpower=pavg

esel,s,mat,,201
powerh
workpeacepower=pavg

el_eff=workpeacepower/realpower
```

```
*if,iiii,eq,1,then

/output,electric_data,dat

*VWRITE
(5x,'Nr',3x,'Runtime,s',5x,'U,V',6x,'V,m/s',8x,'I,A',7x,'P,W',8x,'Pw,W',5x,'el_e
ff',3x,'cosphi')

/output

*endif

/output,electric_data,dat,,append

*VWRITE,iiii,runtime,voltage,vy,current,realpower,workpeacepower,el_eff,cosphi
(2x,F6.0,2x,F8.1,2x,F9.2,2x,F9.6,2x,F9.1,2x,F9.0,2x,F9.0,2x,F7.4,2x,F7.4)

/output

finish
```

The begin of the thermal part

```
/clear
/FILNAME,BATCH_U,1
resume,environment_therm,db
/input,iiii,dat

   /assign,rst,BATCH_U,rth
   /solu
      antype,trans
   allsel

   esel,s,mat,,201
   ldread,hgen,,,,2,,rmg

     esel,s,mat,,201
     esel,a,mat,,501
     nsle

    *if,iiii,eq,1,then
        tunif,20
    *ELSE
      ldread,temp,last,,,2,,rth
    *ENDIF

   esel,all
   nsel,all

nsel,s,loc,x,xr2-eps,xr2+eps
nsel,r,loc,y,yr1-eps,yr2+eps
d,all,temp,40.0

   esel,all
   nsel,all

      neqit,1000
      runtime=input_transient(iiii,3)
      timestep=input_transient(iiii,2)
      time,timestep
   solve
   finish
```

Appendix C

Electrical results

Tabel *Electrical results from the simulations made for D inductor (950A) and C inductor (1550A)*

D inductor				C inductor			
P,W	Pw,W	el_eff	cosphi	P,W	Pw,W	el_eff	cosphi
52266	41207	0,7884	0,138	51343	40961	0,7978	0,1345
62913	51572	0,8197	0,1592	61746	51195	0,8291	0,1551
71417	59798	0,8373	0,1745	70094	59373	0,847	0,1702
77185	65344	0,8466	0,184	75811	64949	0,8567	0,1796
74772	63122	0,8442	0,1826	74186	63402	0,8546	0,1787
51884	40893	0,7882	0,1415	51449	41062	0,7981	0,1391
41905	31076	0,7416	0,117	41437	31157	0,7519	0,1147
36119	25380	0,7027	0,1022	35628	25413	0,7133	0,1
32386	21703	0,6701	0,0925	31773	21597	0,6797	0,09
29607	18934	0,6395	0,0846	28956	18789	0,6489	0,082
28294	17613	0,6225	0,0806	27621	17453	0,6319	0,078
28114	17422	0,6197	0,0799	27418	17245	0,629	0,0772
28586	17888	0,6258	0,0811	27913	17736	0,6354	0,0785
28872	18172	0,6294	0,0819	28262	18083	0,6398	0,0794
28953	18251	0,6304	0,0821	28323	18143	0,6406	0,0795
29002	18299	0,631	0,0822	28372	18192	0,6412	0,0797
29047	18343	0,6315	0,0823	28416	18236	0,6417	0,0798
29090	18386	0,632	0,0824	28458	18277	0,6423	0,0799
29131	18426	0,6325	0,0825	28499	18318	0,6427	0,08
29170	18464	0,633	0,0826	28537	18355	0,6432	0,0801
29207	18500	0,6334	0,0827	28573	18391	0,6436	0,0801
29242	18535	0,6338	0,0828	28607	18425	0,6441	0,0802
29276	18568	0,6342	0,0828	28641	18458	0,6445	0,0803
29307	18598	0,6346	0,0829	28672	18489	0,6448	0,0804
29333	18624	0,6349	0,083	28698	18515	0,6452	0,0804
29359	18649	0,6352	0,083	28723	18539	0,6455	0,0805
29383	18673	0,6355	0,0831	28747	18563	0,6457	0,0805
29407	18696	0,6358	0,0831	28770	18586	0,646	0,0806
29431	18720	0,6361	0,0832	28793	18609	0,6463	0,0807
29455	18743	0,6363	0,0833	28816	18632	0,6466	0,0807

References

Chapter 1

Lupi, S. (2005). 5-Riscaldamento ad induzione. *Appunti di Elettrotermia.*

Chapter 2

2.1 Eurostat - European Commission (2012). *EU Energy in figures – Statistical pocketbook 2012.* Publication Office of the European Union (2012).

2.2 Intelligent Energy Europe (2009). *Energy Efficiency Trends and Policies in the Industrial Sector in the EU-27.* Ademe.

2.3 Eurostat - European Commission. (2011). *Energy Balance Sheets — 2008-2009.*

2.4 EUROFORGE (2011). www.euroforge.org

2.5 Industrieverband Massivumformung. *Basic Knowledge Forgings – Significance, Design, Production, Application.* www.metalform.de.

Chapter 3

Behrens, B. A.(2011). *Resource efficient forging process chain for complicated high duty parts REForCh.* Research for SMEs.

Chapter 4

Behrens, B. A.(2011). *Resource efficient forging process chain for complicated high duty parts REForCh.* Research for SMEs.

4.1 Franz Beneke, Bernard Nacke, Herbert Pfeifer.(2012). *Handbook of Thermoprocessing Technologies: Volume 1*

4.2 Research for SMEs. (2012). *SEVENTH FRAMEWORK PROGRAMME*. Page 45